On Spectrum Sensing for Secondary Operation in Licensed Spectrum

Blind Sensing, Sensing Optimization and Traffic Modeling

MOHAMED HAMID

Doctoral Thesis in
Information and Communication Technology
Stockholm, Sweden 2015

TRITA-ICT-COS-1502
ISSN 1653-6347
ISRN KTH/COS/R--15/02--SE

KTH Communication Systems
SE-100 44 Stockholm
SWEDEN

Akademisk avhandling som med tillstånd av Kungl Tekniska högskolan framlägges till offentlig granskning för avläggande av teknologie doktoralexamen i informations- och kommunikationsteknik fredagen den 13 mars 2015 klockan 13.15 i hörsal 99:131, Hus 99, Högskolan i Gävle, Kungsbäcksvägen 47, Gävle.

Tryck: Universitetsservice US AB

Abstract

There has been a recent explosive growth in mobile data consumption. This, in turn, imposes many challenges for mobile services providers and regulators in many aspects. One of these primary challenges is maintaining the radio spectrum to handle the current and upcoming expansion in mobile data traffic. In this regard, a radio spectrum regulatory framework based on secondary spectrum access is proposed as one of the solutions for the next generation wireless networks. In secondary spectrum access framework, secondary (unlicensed) systems coexist with primary (licensed) systems and access the spectrum on an opportunistic base.

In this thesis, aspects related to finding the free of use spectrum portions - called spectrum opportunities - are treated. One way to find these opportunities is spectrum sensing which is considered as an enabler of opportunistic spectrum access. In particular, this thesis investigates some topics in blind spectrum sensing where no priori knowledge about the possible co-existing systems is available.

As a standalone contribution in blind spectrum sensing arena, a new blind sensing technique is developed in this thesis. The technique is based on discriminant analysis statistical framework and called spectrum discriminator (SD). A comparative study between the SD and some existing blind sensing techniques was carried out and showed a reliable performance of the SD.

The thesis also contributes by exploring sensing parameters optimization for two existing techniques, namely, energy detector (ED) and maximum-minimum eigenvalue detector (MME). For ED, the sensing time and periodic sensing interval are optimized to achieve as high detection accuracy as possible. Moreover, a study of sensing parameters optimization in a real-life coexisting scenario, that is, LTE cognitive femto-cells, is carried out with an objective of maximizing cognitive femto-cells throughput. In association with this work, an empirical statistical model for LTE channel occupancy is accomplished. The empirical model fits the channels' active and idle periods distributions to a linear combination of multiple exponential distributions. For the MME, a novel solution for the filtering problem is introduced. This solution is based on frequency domain rectangular filtering. Furthermore, an optimization of the observation bandwidth for MME with respect to the signal bandwidth is analytically performed and verified by simulations.

After optimizing the parameters for both ED and MME, a two-stage fully-blind self-adapted sensing algorithm composed of ED and MME is introduced. The combined detector is found to outperform both detectors individually in terms of detection accuracy with an average complexity lies in between the complexities of the two detectors. The combined detector is tested with measured TV and wireless microphone signals.

The performance evaluation in the different parts of the thesis is done through measurements and/or simulations. Active measurements were performed for sensing performance evaluation. Passive measurements on the other hand were used for LTE downlink channels occupancy modeling and to capture TV and wireless microphone signals.

Acknowledgements

Looking back, I would confidently say that I am not only glad to accomplish completing this thesis but also the whole path towards this moment was amazingly enjoyable. Therefore, before diving into the technical discussion, I would like to take the opportunity to thank those people whom without their help this journey would have been much tougher and probably unachievable.

First and foremost, I am greatly indebted to my supervisors, Assoc. Prof. Niclas Björsell and Prof. Slimane Ben Slimane. At first for offering me the opportunity to pursue my PhD in such creative and inspiring environment like KTH and HiG. Secondly for keeping encouraging, supporting and trusting in me which helped me a lot to improve myself professionally and , more importantly, as a person. I feel truly fortunate having such two skilled advisors who share without reservation. I am also so thankful to prof. Jens Zander, the head of communication system department at KTH and QUASAR project leader where I have performed considerable part of the work led to this thesis.

Throughout my PhD study, I have collaborated with Prof. Wendy Van Moer, Dr. Kurt Barbé and Prof. Abbas Mohammed and I do appreciate the insights and creative ideas I got from them. I would also like to thank Dr. Ki Won Sung for reviewing this thesis and providing valuable comments and insights. Many thanks goes to Assoc. Prof. Octavia Dobre for accepting coming all the way from Canada to be my opponent in the Doctoral dissertation. Special thanks goes to the members of the grading committee: Prof. Hans-Jürgen Zepernik, Prof. Lars K. Rasmussen, Dr. Muhammad Imadur Rahman and Assoc. Prof. José Chilo.

During these years, many people have been so helpful with the administrative and paper work in both HiG and KTH, I do thank them all and special thank goes to Sarah Winther, CoS department administrator at KTH.

I would also like to thank my friends and colleagues in the Electronics group at HiG for creating such comfortable and inspiring working environments. Particularly, I would like to thank the former and current PhD students: Dr. Per Landin, Dr. Charles Nader, Dr. Prasad Sathyaveer, Dr. Javier Ferrer Coll, Efrain Zenteno, Shoaib Amin. Mahmoud Alizadeh, Rakesh Krishnan, Nauman Masud, Indra Nyoman and Usman Haidar. Guys, our enjoyable discussions in (what so ever) will remain with me. I am also thankful to Elsiddig Elmokashfi and Ashraf Widaa for all the support and the fruitful discussions we have had.

Outside HiG and KTH, I have always been surrounded by many friends who were there whenever needed, among those are the rocks of 2000 batch, Electrical Engineering, U of K, "Kharib 00". Guys, no matter how far are you, you have always been the closest friends I consult, share all the moments with and look forward to catch up with. I will never ever forget the support and the moments I have shared with the Sudanese society in Gävle

My parents Molana Hamid and Ihsan and my grandma, Haboba Alsara, I know that it wasn't easy for you to tolerate the absence of your son all this time, even though, you haven't stopped your countless support and you kept praying for my success. My siblings, Sara, Abdo, Khalid and Hind, thanks for sharing happiness in the toughest times. Finally, my other half Zeinab and our little Hamid, I am so thankful for all the happiness you have brought to my life.!

Contents

List of Tables

List of Figures

List of Acronyms & Abbreviations

2EMC	2-stage ED-MME Combined detector
3GPP	3rd Generation Partnership Project
AIC	Akaike Information Criterion
BS	Base Station
CCDF	Complementary Cumulative Distribution Function
CDF	Cumulative Distribution Function
CR	Cognitive Radio
DSA	Dynamic Spectrum Access
ECC	Electronic Communication Committee (in Europe)
ED	Energy Detector/ Detection
EIRP	Equivalent Isotropic Radiated Power
ETSI	European Telecommunications Standards Institute
FBS	Femto-cell Base station
FCC	Federal Communications Commission (in the US)
FM	Frequency Modulation
FSA	Fixed Spectrum Access
ICA	Independent Components Analysis
IEEE	Institute of Electrical and Electronics Engineers
iid	independent identically distributed
ISM	Industrial, Scientific and Medical band

LTE	Long Term Evolution
MBB	Mobile Broadband
MBS	Macro-cell Base station
MDL	Minimum Descriptive Length
MME	Maximum-Minimum Eigenvalue detection
MO	Mutual Operation
MS	Mobile Station
MUSIC	Multiple Signal Classification
NMSE	Normalized Mean Square Error
NU	Noise Uncertainty
Ofcom	Office of communication (in the UK)
OSA	Opportunistic Spectrum Access
PAD	Personal Digital Assistant
PC	Personal Computer
PDF	Probability Distribution Function
PSD	Power Spectral Density
PU	Primary User
PV	Probabilistic Validation
QoS	Quality of Service
RF	Radio Frequency
RMT	Random matrix Theory
ROC	Receiver Operating Characteristics
RTSA	Real Time Spectrum/Signal Analyzer
RV	Random Variable
SA	Spectrum/Signal Analyzer
SCM	Sample Covariance Matrix
SD	Spectrum Discriminator

SDR	Software Defined Radio
SE43	Spectrum Engineering group (within the ECC)
SG	Signal Generator
SINR	Signal to Interference plus Noise Ratio
SIR	Signal to Interference Ratio
SNR	Signal to Noise Ratio
SSOH	Sensing Overhead
SU	Secondary User
SUF	Spectrum Utilization Factor
TVWS	TV White Space
UHF	Ultra-High Frequency
UMTS	Universal Mobile Telecommunications System
UOP	Unexplored Opportunities
UWB	Ultra Wideband
VHF	Very High Frequency
WBAN	Wireless Body Area Network
WCDMA	Wideband Code Division Multiple Access
WiFi	Wireless Fidelity
WLAN	Wireless Local Area Network
WMAN	Wireless Metropolitan Area Networks
WPAN	Wireless Personal Area Network
WRAN	Wireless Regional Area Network
WWAN	Wireless Wide Area Network

Part I

Comprehensive Summary

Chapter 1

Introduction

1.1 Background

In 1895 Marconi succeeded to transmit the first wireless signal ever using Maxwell's theory. Six years later, in 1901, Marconi himself managed to send a telegraph message wirelessly through the Atlantic as a launch of what is known as radio telegraphy. Since then, wireless transmission has been continuously evolving and new wireless advances have been appearing including broadcasting of audio and video, walkie-talkies, satellite communications, commercial cellular phones, personal communications, multimedia communications and mobile broadband (MBB) services. In general, in today's modern societies, communicating wirelessly is deeply rooted in our daily life. Having that foundation in our need to exchange information, reflects how difficult it is to imagine the globe without wireless systems.

By having all these wireless technologies, the wireless landscape is ranging from a networks that covers thousands of kilometres known as a wireless wide area network (WWAN) to a network that transfers signals within a human body refereed to as a wireless body area network (WBAN). In between, there exist also wireless regional area networks (WRAN), wireless metropolitan area networks (WMAN), wireless local area networks (WLAN) and wireless personal area networks (WPAN). Together with the coverage, another dimension of this landscape is the capacity which goes inversely proportional to the coverage area. Moreover, capacity has been more concerned about with the time progression.

Mobile operators have started with voice communication as their basic service. Thereafter, data communications take over and have been dominating mobile services more and more. Fig. 1.1 depicts the monthly global mobile traffic for voice and data since 2010 with a forecast up till 2018. Fig. 1.1 exhibits the exponential growth of data traffic termed as data tsunami faced by mobile broadband services providers. However, there will be a point where this exponential growth in data traffic is clipped by the availability of infrastructure and resources. One of these resources is the usable electromagnetic radio spectrum below 6 GHz.

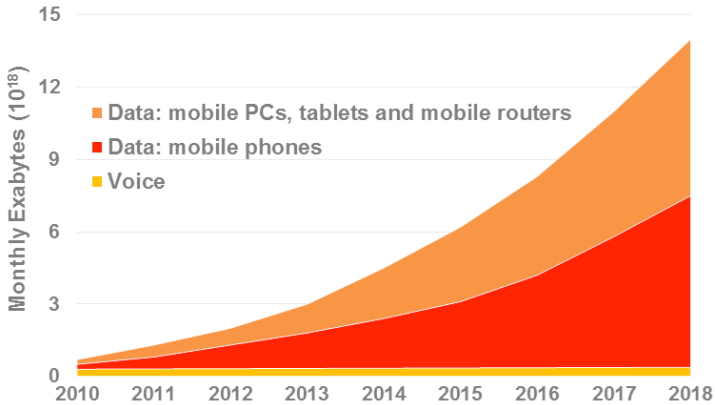

Figure 1.1: Monthly global mobile voice and data traffic, 2010-2018 [1].

One solution to overcome this resources shortage is to use portion of the radio spectrum above 6 GHz. This solution is motivated by the property of the availability of more bandwidth in higher spectrum bands and in return capability of handling higher data rates. In this regard, communicating using the frequencies around 60 GHz has emerged and standardized as a promising technology for multi-gigabit short range links [2, 3]. However, operating in high frequencies is costly in terms of power and hardware needs. Therefore, other alternatives are still needed as complements of opening up new bands. Approaching towards more distributed networks architecture is also an alternative solution for providing higher data rates. However, more distributed networks still need more resources in terms of radio spectrum. Therefore, the need of more radio spectrum is a bottleneck. Accordingly, better radio spectrum reuse seems to be a convincing solution.

Linked to the feasibility of improving the radio spectrum usage, several studies, initiated by the US regulator Federal Communications Commission (FCC), have shown that the frequency spectrum is underutilized and inefficiently exploited, some bands are highly crowded, at some day hours or in dense urban areas, while others remain poorly used. This paradox led the regulators worldwide to recognize that the traditional way of managing the electromagnetic spectrum, called fixed spectrum access (FSA), in which the licensing method of assigning fixed portions of spectrum, for very long periods, is inefficient [4–6].

Among the efforts taken by regulators worldwide, in order to achieve better usage of spectrum is the introduction (promotion) of secondary markets. Besides the promotion for secondary markets, we are currently experiencing rapid evolutions of software defined radio (SDR) techniques. Such techniques allow reconfigurable wireless transceivers to change their transmission/reception parameters, such as the operating frequency that can be modified over a very wide band, according to the network or users' demands. The efforts taken by regulators in order to make better

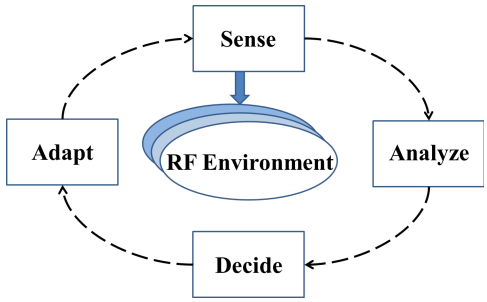

Figure 1.2: CR cycle basic functionalities.

usage of spectrum, in particular the promotion for secondary market, together with the rapid evolution of the SDR techniques, have led to the development of cognitive radio (CR) systems. The term cognitive radio was firstly introduced by J. Mitola in 1999 [7]. Generally, CR refers to a radio device that has the ability to sense its radio frequency (RF) environment and modify its spectrum usage based on what it detects. In short, CR device senses the RF environment, analzses the resources availability, decides on changing its operation parameters and finally adapts to the changes it makes. Fig. 1.2 shows the basic functionalities of the CR cycle. To make it omnipresent, regulators and standardization bodies have been putting policies and standards concerning CR and coexistence of secondary users (SU) with primary users (PU). Among the leading regulation bodies in CR arena is the FCC. In 2010, the FCC released a report that allows secondary operation in the UHF terrestrial TV band in what so called TV white space (TVWS) [8]. In the UK, the Office of communication (Ofcom) has followed the FCC and opened up the first TVWS for secondary operation in Europe [9]. In Europe also, the Electronic Communication Committee (ECC) formed the Spectrum Engineering group (SE43) which is responsible for regulating the license exempt access to the licensed bands [10].

Similar to regulators, industry partners have been standardizing secondary access to the primary users bands. Being a leader in wireless industry standardization, Institute of Electrical and Electronics Engineers (IEEE) has released many standards concerning secondary operation, among those, the 2011 released standard by the working group 802.22 [11]. This standard regulates the deployment of WRAN in TVWS. More IEEE standards for secondary operation have been either released or under preparation such as IEEE 1900 group of standards which is responsible for standardizing the new technologies for next generation radio and advanced spectrum management [12]. A detailed survey on the IEEE standards in CR and coexistence issues is found in [13].

1.2 Spectrum Sharing

Spectrum sharing is a terminology used for the concurrent access of spectrum in a specific geo-location at a specific time by multiple independent entities using mechanisms other than the multiple access techniques [14]. Spectrum sharing can be classified differently depending on the consideration of the classification. Below are three spectrum sharing classifications with different concerns found in the literature.

Spectrum Access Rights Classifications

This classification considers the rights of accessing the shared spectrum. this classification divides spectrum sharing systems into two categories described below [14].

Horizontal sharing: All sharing entities are equally illegible to access the spectrum. The ownership of the spectrum is the same as well for the different entities. This type of spectrum sharing is applicable in both licensed and unlicensed spectrum. An example of licensed spectrum horizontal sharing is different mobile stations (MS) accessing the uplink cellular spectrum. On the other hand, a WiFi access point sharing a portion of the 2.4 GHz industrial, scientific and medical (ISM) band with a microwave oven is an example of horizontal unlicensed spectrum sharing.

Vertical sharing: This type of sharing is also called dynamic spectrum access (DSA). Here, sharing systems have different rights to access the spectrum. Under the vertical spectrum sharing framework, the spectrum owned by the licensed PU can be shared by a non-licensee SU. SUs can be dynamically allocated the empty frequencies within the licensed frequency band, according to their requested quality of service (QoS) specifications. SUs have to share the spectrum with associated constrains that assure PU protection such as the transmission power limits.

Access Technology Classification

Based on the spectrum access technology, spectrum sharing is categorized in [15] into overlay, underlay and interweave sharing models as descried below.

Underlay sharing: Is the spectrum sharing approach when the SUs coexist with the PU regardless of the PU existence or absence. However, accumulative SUs transmission has to be kept below a specific interference limit. This definition of underlay spectrum sharing implies restrictions on the SU transmission power. Most noticeably, ultra wideband (UWB) systems follows underlay spectrum sharing model where the UWB signal is spread over a very wide portion of spectrum that can be owned by many PUs with a very low transmission power.

Overlay sharing: Here SUs are allowed to coexist with the PU as in underlay sharing model with different constrains. With overlay sharing, the PU performance is not only maintained with no degradation caused by SUs but also can be enhanced with the aid of SUs. One approach to enhance the PU performance by coexisting SU is to use network coding where SUs act as relay nodes between PU weakly connected nodes [16].

Interweave sharing: With interweave spectrum sharing, PU is the absolute owner of the spectrum and have the right to access it exclusively whenever needed. Accordingly, SUs are allowed to access the spectrum when the PU is inactive. Moreover, SUs are required to vacate the band when the PU resumes its operation. Therefore, interweave spectrum sharing model is also called opportunistic spectrum access (OSA).

Cooperation Classification

Spectrum sharing is also classified based on whether sharing systems cooperate with each other or not. This classification is directly involved in system design [17].

Coexistence sharing: With coexistence spectrum sharing, the participating systems try to avoid mutual harmful interference with no common protocol or signalling. One approach to mitigate mutual interference is employing CR capabilities including transmission parameters adjustment.

Cooperative sharing: Cooperative spectrum sharing is the sharing model when the sharing devices communicate using the same administrative protocol. Cooperation among the participating systems is obligatory aiming at mitigating mutual interference. The joint benefit is maximized when adopting cooperative sharing with extra overhead of having common supported protocol(s).

The sharing model considered in the studies of this thesis is *vertical, interweave* and *coexistence* sharing model and for that DSA and OSA are used interchangeably. To adopt DSA, SU needs at first to locate and later utilizes the usable free of use spectrum. This free of use spectrum is called spectrum hole or spectrum opportunity, these two terms are interchangeably used. Spectrum hole is defied in [18] as *"a band of frequencies assigned to a primary user, but, at a particular time and specific geographic location, the band is not being utilized by that user"*. This definition imposes a multi-dimensional spectrum awareness concept since a spectrum hole is a function of frequency, time and geo-location [19]. Figure 1.3 depicts the concept of spectrum hole.

According to the literature, one of three approaches can be used to find the spectrum opportunities [20]. Those three approaches are: spectrum sensing[1], geo-

[1]Spectrum sensing is called signal detection also. Therefore, throughout this thesis sensing and detection are used interchangeably.

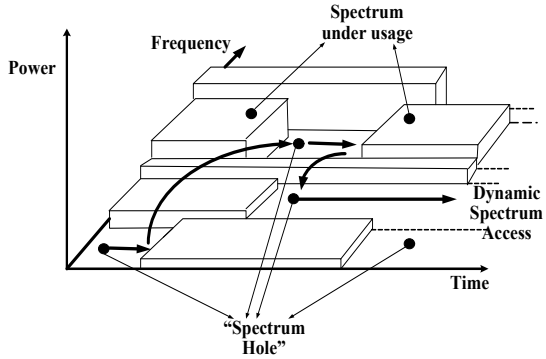

Figure 1.3: Spectrum hole concept.

locations databases and beacon signals. These three approaches are described below.

Spectrum sensing: SU scans across the usable spectrum and identify the spectrum holes using one of the spectrum sensing techniques, [19, 21]. There are many of those techniques with different complexity and reliability extent, Section 1.3 provides a brief review of the sensing techniques in the literature.

Geo-location databases: Spectrum opportunities with their associated constrains are reported in an accessible database by SUs. The geo-location databases based spectrum opportunities are suitable when the PU usage pattern is fixed or varies slowly over time [22]. Therefore, the TV broadcasting and the radar systems are potential PUs to adopt the geo-location databases for spectrum opportunities [23–29]. This is - of course - after taking into the consideration the inefficient use of the spectrum assigned for the TV broadcasting and radar systems. The main concern when building the geo-location databases spectrum opportunities is protecting the PU from harmful interference [30].

Beacon signals: To determine the spectrum opportunities using the beacon signals method, SUs detect PUs' signatures through receiving a beacon signal from those PUs [31]. Beacon signals based spectrum opportunities approach attracts less attention since it costs burden on PUs and requires more resources in terms of standardized channel.

In [20] spectrum sensing, geo-location databases and beacon signals have been compared concerning different aspects. Table 1.1 summarizes the comparative study held in [20]. Rest of this thesis treats aspects in using spectrum sensing as an enabler of finding spectrum holes.

Table 1.1: Spectrum sensing, geo-location database and beacon signals comparison

	Main responsibility	Infrastructure cost	Transceiver complexity	Positioning	Internet connection	Standardized channel	Continuous monitoring
Spectrum sensing	SU	Low	High	No	No	No	Yes
Geo-location DB	PU	High	Low	Yes	Yes	No	No
Beacon Signals	PU	High	Low	No	No	Yes	No

1.3 Spectrum Sensing Techniques

In the literature there are many spectrum sensing enabling algorithms with different complexity and reliability extent, following is a brief overview of the most common spectrum sensing techniques.

Energy Detection

The detector performs spectrum sensing by calculating the signal energy and declaring PU existence if this energy exceeds the noise floor level [32]. For energy detection a priori knowledge about noise energy level is necessary and its uncertainty degrades the detector performance [33]. Energy detection procedure is explained in details in Chapter 3.

Feature Detection

These types of detectors exploit certain PU signal properties such as pilots or cyclostationary features to perform the detection [34]. Feature detection requires knowledge about cyclic frequencies of the PU signal. However, this type of detection requires a very accurate synchronization which is difficult to maintain in low signal-to noise ratio (SNR) values [35].

Matched Filtering Detection

With this technique of detection, the received signal is matched filtered with the PU signal and accordingly the existence or absence of the PU is determined [36]. The matched filtering detection relies on the assumption of having Gaussian noise where the matched filtering is the optimal detection technique [37]. For matched filtering detection, perfect knowledge regarding PU signal features including modulation

scheme, pulse shaping and bandwidth is a requirement. Matched filtering detection has the same limitation as feature detection in low SNRs [35].

Waveform Based Sensing

Different communication signals use different known patterns such as preambles, pilots and spreading sequences for specific purposes like synchronization. These known patterns can be used to identify a specific PU signal existence in what so called waveform based sensing [38].

Eigenvalues Based Detection

For spectrum sensing, many techniques have been developed using the eigenvalues or the eigenvectors of the received signal covariance matrix, these techniques include maximum-minimum eigenvalue detection, energy with minimum eigenvalue, maximum eigenvalue detection, generalized likelihood ratio test, scaled largest eigenvalue, John's detection and spherical test. Detailed explanations of these techniques are included in [39–46]. Section 3.2 presents in details one of these eigenvalues based detection techniques, namely maximum-minimum eigenvalue detection.

Basic Comparison of Sensing Techniques

Different sensing techniques achieve different levels of reliability with different complexities and different grades of information needed about PU signal. Fig. 1.4 shows a basic comparison concerning reliability, complexity and the amount of information needed about the PU signal of the basic sensing techniques presented in this Section. Fig. 1.4 is generated with an aid from [19].

1.4 Challenges in DSA

In this section different challenges faced by DSA are briefly overviewed. As a transition to the next section, the challenges directly or indirectly related to the issues addressed in this thesis are covered in more details. Challenges in DSA arena can be categorized into business, regulatory and technical challenges [47] as exhibited by Fig. 1.5 and elaborated more on hereafter.

Regarding business challenges, the model of DSA still lacks a lot of quantitative evaluation methodologies for many factors including technology availability, infrastructure modifications and deployment costs. These undefined factors make the economical revenue uncertain which in return leads to reluctance or at least hesitation from industry to invest in DSA. Moreover, the uncertainty of new players appearance discourage the industry to get in DSA.

From regulators point of view, motivating the licensee operators to share their spectrum seems a fundamental challenge. Therefore, incentive regulatory framework for DSA to encourage license holders to adopt DSA is needed. Furthermore,

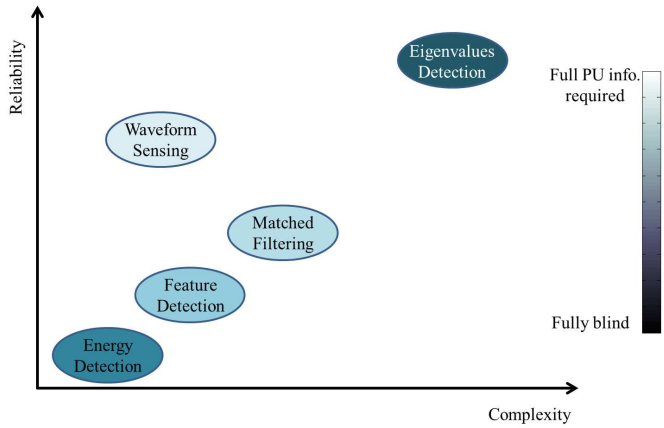

Figure 1.4: Sensing techniques comparison.

enforcement of regulation with more dynamicity in the system that implies more violations is a challenge for the regulators. In addition, regulatory framework has to consider both PU protection and SU performance.

For the technical challenges, many aspects are involved. Following are the technical challenges being discussed the most in the literature. At first, the impact of secondary operation on PU performance is a challenge faced by DSA. Another technical challenge faces DSA is the scalability extent of the deployed secondary systems. Associated with the scalability issues, developing sharing mechanisms that guarantees acceptable quality of services for not only PUs but also coexisting SUs is a big technical challenge in DSA.

Fetching and disseminating spectrum availability knowledge is a challenge that attracts most of the research within DSA. A preliminary challenge is to decide which approach among spectrum sensing, geo-location database or beacon signals to use as presented in Section 1.2, Moreover, which bands are suitable for which approach is an attractive research question. DSA technical challenges are many and very branched which are surveyed in [15, 47]. As the main area where this thesis contributions fall, challenges in spectrum sensing are divided into the challenges shown by Fig. 1.5 and covered in more details in the upcoming parts of this Chapter.

1.5 Problem Formulation and Contribution Overview

This section acts as a "high level" problem formulation of the topics addressed in the thesis with an overview of the associated thesis contribution. The high level problem formulation is presented in a group of *research questions* addressed in the thesis. The contributions of the thesis are led by these research questions and spread

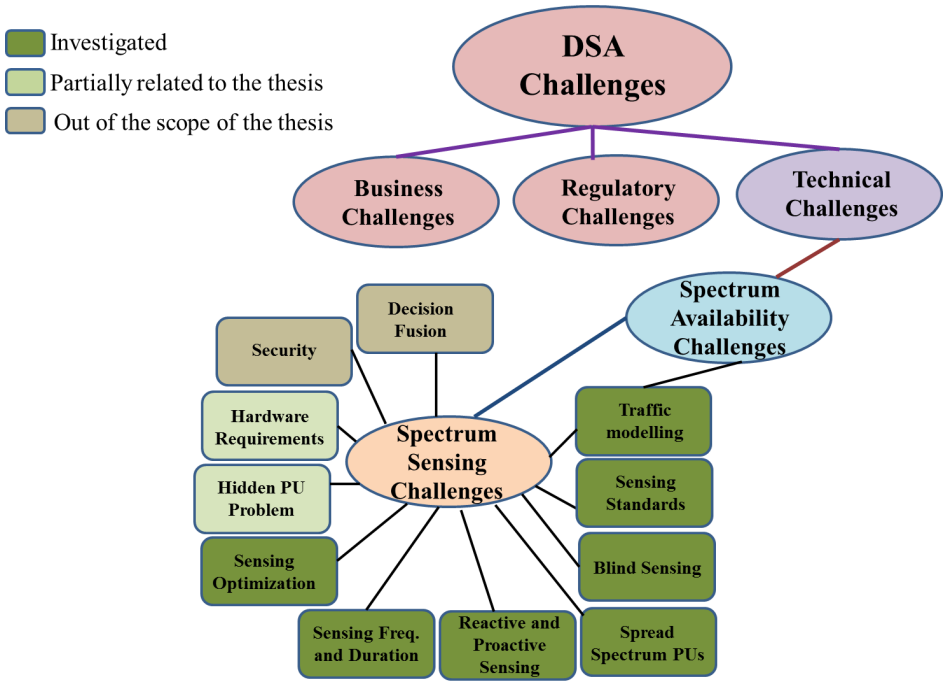

Figure 1.5: Challenges in DSA associated with the thesis contributions.

in ten publications indexed as **Paper I** to **Paper X** according to their contributions appearance in the thesis. For the sake of coherency, some parts of some publications are skipped and some parts of some other publications are presented in different parts of the thesis. Moreover, contributions included fully or in part in more than one publications are presented once. Linked to the spectrum sensing challenges shown in Fig. 1.5, these publications contributes in each challenge differently. Fig. 1.6 maps the publications contributions to these challenges and research questions. Following addressed challenges are ordered in accordance with the significances of the contributions .

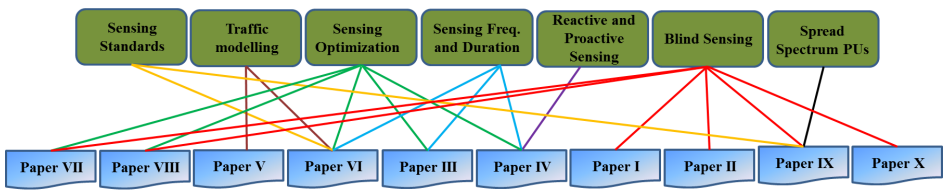

Figure 1.6: Challenges-contributions connections map.

Blind Sensing

Spectrum sensing can be performed using a priori knowledge about either the noise floor level or the PU signal pattern. However, this knowledge may not be available in most cases. Consequently, a sensing technique for which no information about neither the noise energy nor the PU signal are available is needed. Such a technique is called blind sensing technique [39, 40].

Related Work

The need for sensing the spectrum blindly is being widely realized for CR. In [48] the authors proposed a blind spectrum sensing technique relies on the goodness of fit to the t-distribution when the noise is uncertain. In [49] independent components analysis (ICA) is used to blindly perform the spectrum sensing. In [50] information theocratic criteria is proposed for blind spectrum sensing by means of estimating the source signals in a received mixture. In [51] a blind spectrum sensing technique based on high order statistics is developed. Using of high order statistics makes use of the fact that for a white Gaussian noise the third and higher moments are zeros. Eigenvalues based spectrum sensing techniques have been proposed as blind sensing techniques [39–46]. More related work is revisited in the context of the contributions reported in Chapter 3 and Chapter 5.

With a comprehensive literature review, one would realize that following research questions are still needed to be investigated.

- **RQ1:** Are there mathematical techniques that can be used for developing reliable, "not so complicated" and non-parametric blind sensing technique?
- **RQ2:** How simplicity and blindness can be traded off and gained simultaneously?

These two research questions direct the thesis contribution in blind spectrum sensing.

Contribution

The thesis contributes in blind spectrum sensing aspects by the materials included in **Paper I**, **Paper II**, **Paper VII**, **Paper VIII**, **Paper IX** and **Paper X** as follows

Paper I: M. Hamid, K. Barbé, N. Björsell and W. Van Moer, Spectrum sensing through spectrum discriminator and maximum-minimum eigenvalue detector: A comparative study, *IEEE International Instrumentation and Measurement Technology Conference (I2MTC)*, May, 2012.

In this paper we present a new spectrum sensing technique for cognitive radios based on discriminant analysis called spectrum discriminator and compare it with

the maximum-minimum eigenvalue detector as they are both blind sensing techniques. The main difference between both techniques is that the spectrum discriminator is a non-parametric technique while the maximum-minimum eigenvalue detector is a parametric. The comparative study between both techniques has been done based on two performance metrics: the probability of false alarm and the probability of detection. For the spectrum discriminator an accuracy factor called noise uncertainty is defined as the level over which the noise energy may vary. Simulations are performed for different values of noise uncertainty for the spectrum discriminator and different values for the number of received samples and smoothing factor for the maximum minimum eigenvalue detector.

Paper II: M. Hamid, N. Björsell, W. Van Moer, K. Barbé and S. Ben Slimane, Blind spectrum sensing for cognitive radios using discriminant analysis: A novel approach, *IEEE Transaction on Instrumentations and Measurements, 2013.*

This paper is an extension of **Paper I**. The extensions include using the probabilistic validation feature to overcome the limitations of the discriminant analysis as an alternative approach with defining noise uncertainty. Moreover, the comparative studies include energy detector with inclusion of sensing time in the comparisons. The spectrum discriminator has been further developed to a peel off technique where different PUs can be detected. The peel off technique performs wideband sensing. The performance of the peel off technique has been tested on simulations and experimentally verified.

Paper VII: M. Hamid and N. Björsell, Maximum-minimum eigenvalues based spectrum scanner for cognitive radios, *IEEE International Instrumentation and Measurement Technology Conference (I2MTC)*, May, 2012.

The fundamental problem addressed in this paper is the inability of using maximum-minimum eigenvalue detection with ordinary time domain filtering where the white noise becomes colored. The solution proposed here is based on frequency domain rectangular filtering. By frequency domain rectangular filtering we take the spectral lines inside each sub-band and throw out the rest. After doing the frequency domain rectangular filtering, the corresponding time domain signal are generated and injected into to the maximum-minimum eigenvalue detector. An experimental verification has been performed and the obtained results show that the technique is implementable with a performance better than the energy detector as a reference technique in terms of the probability of detection when both techniques are designed to achieve the same probability of false alarm.

Paper VIII: M. Hamid, N. Björsell and S. Ben Slimane, Signal bandwidth impact on maximum-minimum eigenvalue detection, *IEEE Communications Letters, 2015.*

The impact of the signal bandwidth and observation bandwidth on the detection

performance of the maximum-minimum eigenvalue detector is studied in this paper. The minimum descriptive length (MDL) criterion is used to split the signal and noise corresponding eigenvalues which are then fitted to different Marchenko Pastur densities considering Gaussian signals. The optimum ratio between the signal and the observation bandwidth is analytically proven to be 0.5 when reasonable values of the system dimensionality are used. The analytical proof is verified by simulations.

Paper IX: M. Hamid, N. Björsell and S. Ben Slimane, Energy and eigenvalue-based combined fully-blind self-adapted spectrum sensing algorithm, *IEEE Transactions on Vehicular Technology, under revision.*

In this paper, a comparison between energy and maximum-minimum eigenvalue detectors is performed. The comparison has been made concerning the sensing complexity and the sensing accuracy in terms of the receiver operating characteristics (ROC) curves. The impact of the signal bandwidth compared to the observation bandwidth is studied for each detector. For the energy detector, the probability of detection increases monotonically with the increase of the signal bandwidth. For the maximum-minimum eigenvalue detector, the findings of **Paper VIII** are adopted and verified. Based on the comparisons outcomes, a combined two-stage detector is proposed, and its performance is evaluated based on simulations and measurements using real-life signals. The combined detector achieves better sensing accuracy than the two individual detectors with a complexity lies in between the two individual complexities. The combined detector is fully-blind and self-adapted as the maximum-minimum eigenvalue detector estimates the noise and feeds it back to the energy detector. The performance of the noise estimation process is evaluated in terms of the normalized mean square error (NMSE).

Paper X: M. Hamid, N. Björsell and S. Ben Slimane, Sample covariance matrix eigenvalues based blind SNR estimation, *IEEE International Instrumentation and Measurement Technology Conference (I2MTC)*, May, 2014.

In this paper, the noise estimation algorithm developed in **Paper IX** is used to blindly estimate the received SNR. After estimating the noise power, the signal power is accordingly estimated using the knowledge of the mixture power. The experimental results are judged using the NMSE between the estimated and the actual SNRs. The results show that, depending on the value of the received vectors size and the number of received vectors, the NMSE is changed and down to -55 dB NMSE can be achieved for the highest used values of the system dimensionality.

Sensing Parameters Optimization

In this thesis different objectives are considered for optimizing the performance of energy and maximum-minimum eigenvalue detectors. For energy detector, the sensing time and periodic sensing intervals are optimized with an objective of max-

imizing the sensing accuracy or the SU throughput. For maximum-minimum eigenvalue detector, the detection performance is enhanced by means of frequency domain rectangular filtering proposed in **Paper VII**. Moreover, the optimum occupation/detection bandwidth ratio analysis carried out in **Paper VIII** is an optimization problem solved to improve the sensing accuracy of the maximum-minimum eigenvalue detector. As shown by Fig. 1.6, the contributions in **Paper VII** and **Paper VIII** are overlapped between blind sensing and sensing optimization areas. Moreover, the rest of the publications contribute in sensing optimization concerning sensing frequency and duration optimization. Hence, sensing optimization and sensing frequency and duration challenges are presented as one part hereafter.

Related Work

In [52] the authors proposed a sensing time optimization and channels ordering approach based on maximizing the SU throughput. The authors of [53] include a penalty term in the SU reward function, this penalty term compensate for the sensing quality in terms of the probability of miss detection which is the probability of miss detecting the PU signal when it exists. In [54] the sensing time and periodic sensing intervals are optimized concerning mitigating the interference with the PU and maximizing the transmission efficiency. Optimizing the sensing time aiming at minimizing the energy consumption in a cooperative sensing framework is explored in [55]. Throughput based sensing parameters setting is investigated in [56] where sensing time is set aiming at maximizing the SU throughput. The contributions are contrasted against the related work in Chapter 4.

As continuations of what has been done in the literature regarding sensing parameters optimization, the thesis contributes by addressing the following research questions

- **RQ3:** What are the objectives of parameters setting concerning PU and SU performance?
- **RQ4:** How frequent the sensing is performed with spectrum opportunities utilization considerations?

Contribution

Sensing time and periodic time interval optimization related contributions are included in **Papers III, Paper IV** and **Paper VI** as explained below.

Paper III: M. Hamid and N. Björsell, A novel approach for energy detector sensing time and periodic sensing interval optimization in cognitive radios, *Proceedings of the 4th International Conference on Cognitive Radio and Advanced Spectrum Management(CogART)*, Oct., 2011.

In this paper a new approach of optimizing the sensing time and periodic sensing

interval for energy detectors has been explored. This new approach is built upon maximizing the probability of right detection, captured opportunities and transmission efficiency. The probability of right detection is defined as the probability of having no false alarm and correct detection. Optimization of the sensing time relies on maximizing the summation of the probability of right detection and the transmission efficiency while optimization of periodic sensing interval is subjected to maximizing the summation of the transmission efficiency and the captured opportunities. The optimum sensing time and periodic sensing interval are dependent on each other, hence, iterative approach to optimize them is applied until they both converge.

Paper IV: M. Hamid, A. Mohammed and Z. Yang, On spectrum sharing and dynamic spectrum allocation: MAC layer spectrum sensing in cognitive radio networks, *IEEE International Conference on Communications and Mobile Computing (CMC)*, China, Apr., 2010.

In contrast to **Paper III**, this paper considers a heterogeneous multi-channel system where the main concern is to improve the utilization of the opportunities in the whole system rather than the individual channels. Therefore, spectrum utilization factor is introduced and used as a performance metric. This paper consists of other contributions regarding reactive and proactive sensing and idle channel search delay which are out of the scope of the thesis.

Paper VI: M. Hamid, N. Björsell and S. Ben Slimane, Downlink throughput driven channel access framework for cognitive LTE femto-cells, *IEEE Transactions on Wireless Communications, Submitted*.

In this paper, a downlink channel access framework for cognitive long term evolution (LTE) femto-cell is developed. The framework objective to maximize the downlink throughput of the femto-cells. Energy detection is used by the cognitive femto-cells to find the free of use channels. The occupancy of the LTE downlink channels is empirically modeled using exponential distributions mixture. The throughput is maximized by compromising the transmission efficiency, the explored spectrum opportunities and the interference from the macro-cell obtained using the LTE signals propagation models adopted in the 3GPP standards. The obtained results show that the maximum achievable throughput is maximized by setting the proper periodic sensing intervals.

PU Traffic Modeling

For reliable performance analysis of secondary systems, different PUs activities on the licensed channels are needed to be modeled. Some PUs' traffic patterns are highly predictable or slowly varying over time like TV and radars systems. On the other hand, for some other PUs, the traffic considerably varies over time such as cellular systems. This part of the thesis targets empirical modeling of LTE macro-

cell downlink channel occupancy which is used in the context of spectrum sharing as a PU in LTE cognitive femto-cell scenario investigated in **Paper VI**.

Related Work

Many studies have been carried out to characterize the cellular channel occupancy statistical distribution. In [57], it is shown that mobile telephony channel occupancy can be approximated by exponential distribution. A great advantage of the exponential distribution is the traceability in finding analytical solutions for optimization problems. Therefore, exponential distribution has been intensively used to model cellular channel occupancy, see [56] as an example. Nevertheless, many research findings concluded poor similarity between exponential distribution and empirical data [58]. One of the main disagreements between exponential distribution and empirical data is the heavy tail behaviour for the empirical channel occupancy which is not properly characterized by exponential distributions. Therefore, some heavy tail distributions are used as alternatives to model the cellular channel occupancy, among which, the log-normal distribution is found to better fit the empirical data [59, 60].

In spite of the massive amount of research being done in PU traffic model, the literature still lacks an answer to the following research question which shapes the thesis contribution in PU traffic modeling

- **RQ5:** Are there exist better statistical models to characterize the PU channel occupancy and preserve the ease for optimization problems analytical solutions with exponential distributions?

Contribution

The thesis contribution in PU traffic modeling is included in **Paper V** described in brief below

Paper VI: **M. Hamid**, N. Björsell and S Ben Slimane, Empirical statistical model for LTE wownlink channel occupancy, *Springer Journal of Wireless Personal Communications, Submitted*.

This paper develops an empirical statistical channel occupancy model for downlink LTE cellular systems. The model is based on statistical distributions mixtures for the holding times of the channels. Moreover, statistical distribution of the time when the channels are free is also considered. The data is obtained through an extensive measurement campaign performed in Stockholm, Sweden. Two types of mixtures are considered, namely, exponential and log-normal distributions to fit the measurement findings. The log-likelihood of both mixtures is used as a quantitative measure of the goodness of fit. Moreover, finding the optimal number of linearly combined distributions using the Akaike information criterion (AIC) is investigated. The results show that good fitting can be obtained by using a group

of either exponential or log-normal distributions linearly combined. Even though, the fitting is done for a representative case with a tempo-spatial consideration, the model is yet applicable in general for LTE and other cellular systems in a wider sense.

The idea of using discriminant analysis for blind spectrum sensing was initiated by Wendy Van Moer and Kurt Barbé. The author of this thesis was the leading contributor in **Paper I** and **Paper II** who built up the system model, performed the simulations and the measurements, analysed the results jointly with the other co-authors. The other co-authors took part in refining the manuscripts and pointing the focus and directions of the two papers. For the rest of the included publications, the author of this thesis was the main contributor who formulated the problems, performed the associated analytical and experimental work. The results were analyzed jointly with the other co-authors. The findings are presented according to the insights given by the other co-authors.

Other Addressed Challenges

As illustrated by Fig. 1.6, the contributions of this thesis fall in other challenges in spectrum sensing as elaborated more in this subsection.

Regarding *sensing some standardized systems*, **Papers VI** and **IX** provide contributions as follows. In **Paper VI** a defined sharing scenario is investigated, that is, LTE cognitive femto-cells where the periodic sensing is performed with the aim of maximizing the downlink femto-cell throughput. In this scenario, one of the distinctions regarding spectrum sensing is that there is no consideration of miss detecting the PU or the macro-cell signal as the sensing is done within the cell serving area where the signal power is by no means undetectable. Moreover, the 3GPP adopted propagation models for both outdoor and indoor LTE signals are used. In **Paper IX**, measured TV and wireless microphone signals are plugged into a two-stage combined fully blind detector. Sensing TV and wireless microphone signals is included as a part of IEEE 802.22 standard of WRAN sharing spectrum in the UHF broadcasting band [11].

Even though **Paper III** is partially included in this thesis concerning periodic sensing intervals optimization in a multi-channel system, yet it includes contribution in investigating the idle channel search delays for both *reactive and proactive sensing* and the trade off when applying one of them.

Spread spectrum PU detection is a challenging problem as these PU signals are difficult to be distinguished from the noise for two reasons. At first, they have low power spectral density which allows them to be hidden under the noise. Secondly, spread spectrum signals are Gaussian signals. In **Paper IX** this problem has been addressed in two manners. Being spread over wide bandwidth with low power spectral density is treated by the second stage maximum-minimum eigenvalue detector which can handles low power signal and adjust its observation bandwidth in accordance with the findings of **Paper VIII**. Moreover, the noise estimation

performed by the maximum-minimum eigenvalue detector and fed back to the first stage energy detector makes it easier to detect these low power signals. However, a fundamental limit is reached when these spread spectrum PUs signals occupy very wide bandwidth.

Partially Addressed Challenges

As Fig. 1.5 exhibits, two challenges in spectrum sensing are partially related to the thesis contributions, namely, SU hardware requirements and hidden PU problem. Regarding SU (or sensing device) hardware requirements, sensing technique complexity measured in sensing time is directly related to the sensing device hardware complexity needed. Therefore, the thesis gives ideas regarding the required hardware complexity levels for different sensing techniques. Hidden PU problem is a terminology used for weak PU signals or passive primary receivers such as TV receivers. As the ultimate goal of performing blind sensing and optimizing the sensing accuracy is to improve the sensing sensitivity, then the thesis partially contributes in addressing the hidden PU problem.

1.6 Related Materials not Included in the Thesis

The following publications or presentations are not appended in the thesis due to sake of coherency, yet, they are in the same area of study covered by the thesis.

(1) **M. Hamid** and A. Mohammed, MAC layer spectrum sensing in cognitive radio networks, Book Chapter in *Self-Organization and Green Applications in Cognitive Radio Networks*, IGI Global, Jan. 2013.

(2) **M. Hamid**, N. Björsell and A. Mohammed, Iterative optimization of energy detector sensing time and periodic sensing interval in cognitive radio networks, Book Chapter in *Self-Organization and Green Applications in Cognitive Radio Networks*", IGI Global, Jan. 2013.

(3) **M. Hamid** and N. Björsell, Frequency hopping for fair radio resources distribution in TVWS , submitted to *10th International Conference on Cognitive Radio Oriented Wireless Networks and Communications, (CrownCom)*, Qatar, Apr., 2015.

(4) **M. Hamid**, J. Ferrer-Coll, N. Björsell, J. Chilo and W. Van Moer, Multi-interference detection algorithm using discriminant analysis in industrial environments, *39th Annual Conference of the IEEE Industrial Electronics Society, IECON*, Austria, Nov., 2013.

(5) **M. Hamid** and N. Björsell, Power assignment for secondary users operating in TVWS geo-locations database based cognitive radios, poster presentation at *2012 Swedish Communication Technologies Workshop (Swe-CTW)*, Lund, Sweden, Oct., 2012.

(6) W. Van Moer, N. Bjorsell, **M. Hamid**, K. Barbe and C. Nader , Saving lives by integrating cognitive radios into ambulances, *IEEE International Symposium on Medical Measurements and Applications Proceedings (MeMeA)*, Hungary, May, 2012.

(7) **M. Hamid** and N. Björsell, Maximum-minimum eigenvalues based spectrum scanner in GNU radio, *Radio Frequency Measurement Technology Conference (RFMTC)*, Sweden, Oct., 2011.

(8) **M. Hamid** and N. Björsell, Geo-location spectrum opportunities database in radar bands for OFDM based cognitive radios, *IEEE First Global Conference on Communication, Science, Information and Engineering (CCSIE)*, UK, Jul., 2011.

(9) **M. Hamid** and A. Mohammed, MAC layer sensing schemes in cognitive radio networks, poster presentation at *third International Conference on Experiments/ Process/ System Modeling/ Simulation/ Optimization (IC-EpsMsO 09)*, Greece, Jul., 2009.

(10) N. Björsell, **M. Hamid**, J. Kerttula, E. Obregon, M.I. Rahman, Initial report on the tolerance of legacy systems to transmissions of secon-dary users based on legacy specifications, *QUASAR Deliverable D3.1*, Jun., 2010.

(11) **M. Hamid**, J. Kerttula, K. Koufos, M. I. Rahman, L.K. Rasmussen, K. Ruttik, N. Schrammar, E. Stathakis, C. Wang, Refined models for primary system performance as a function of secondary interference", *QUASAR Deliverable D 3.2*, Dec., 2010.

(12) V. Atanasovski , N. Björsell, J. W. Van Bloem, D. Denkovski, L. Gavrilovska, **M. Hamid**, R. Jäntti, S. Kawade, J. Kerttula, M. Nupponen, M. Zahariev, Laboratory test report, *QUASAR Deliverable D 2.5*, Mar., 2012.

(13) A. Achtzehn, T. Alemu, V. Atanasovski, N. Björsell, T. Dudda, L. Gavrilovska, **M. Hamid**, T. Irnich, R. Jäntti, J. Karlsson, J. Kerttula, K. Koufos, J. Kronander, P. Latkoski, R. Malekafzaliardakani, G. Martinez, E. Obregon, A. Palaios, N. Perpinias, M. Petrova, M. Prytz , K. Ruttik, L. Simic , K. W. Sung, Final Report on Models with Validation Results, *QUASAR Deliverable D 5.4*, Jun., 2012.

1.7 Thesis Outline

The thesis is composed of two parts. The first part is a comprehensive summary of the included publications which introduces the theoretical aspects and the findings of the thesis. This part is divided into five chapters. Chapter 2 handles the system model and performance evaluation methodology followed throughout the thesis.

Chapter 3 presents in details energy detection and maximum-minimum eigenvalue detection as the raw materials used in the different contributions of the thesis. Chapter 3 ends with presenting spectrum discrimination based blind sensing with a comparison with the pre-mentioned two techniques. In Chapter 4 the optimizations carried out for both two detectors are included. The fully blind two-stage detector composed of energy and maximum-minimum eigenvalue detectors is covered in Chapter 5. Finally, Chapter 6 concludes the thesis and provides some proposed directions for the future research in related aspects. The second part presents a verbatim version of the included publications.

Chapter 2

System Model and Performance Evaluation

THIS chapter presents the models for the signal and channel access used in the thesis. In addition to, the performance metrics used for performance evaluation and optimization are also introduced in this chapter. The chapter ends with presenting the sensing performance evaluation approaches including evaluation signals and measurements setup.

2.1 Signal Model and Binary Hypothesis Framework

Suppose a received signal, $\mathbf{X}$, which can be either a PU signal, $\mathbf{S}$, bearing noise, $\mathbf{Z}$, or noise only components. In this context, a binary hypothesis framework can be put as

$$\mathbf{X} = \begin{cases} \mathbf{Z} & \mathcal{H}_0 \\ \mathbf{S} + \mathbf{Z} & \mathcal{H}_1 \end{cases}, \tag{2.1}$$

where $\mathcal{H}_0$ is the null hypothesis denoting noise only existence and $\mathcal{H}_1$ is the positive hypothesis denoting signal bearing noise existence.
The main task of spectrum sensing is to declare either $\mathcal{H}_0$ or $\mathcal{H}_1$ from $\mathbf{X}$. $\mathbf{X}$ is composed of L vectors of the time domain received signal with N samples each. Accordingly, $\mathbf{X}$ is an $N \times L$ complex values matrix which is composed as

$$\mathbf{X} = \begin{pmatrix} x_{1,1} & x_{1,2} & \cdots & x_{1,L} \\ x_{2,1} & x_{2,2} & \cdots & x_{2,L} \\ \vdots & \vdots & \ddots & \vdots \\ x_{N,1} & x_{N,2} & \cdots & x_{N,L} \end{pmatrix}. \tag{2.2}$$

$\mathbf{Z}$ and $\mathbf{S}$ can be expressed using the similar notation as $\mathbf{X}$. $\mathbf{Z}$ is a zero-mean Gaussian random process with a variance of σ_z^2 while $\mathbf{S}$ is a zero mean random series with a variance of σ_s^2. Consequently, the SNR denoted as $\gamma_0 = \sigma_s^2/\sigma_z^2$.

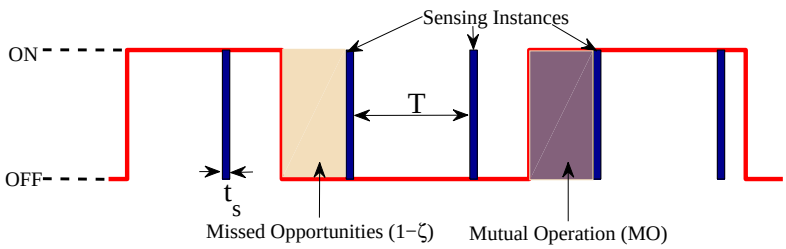

Figure 2.1: Opportunistic channel access model.

2.2 Opportunistic Channel Access Model

The available channel for secondary access are modeled as a two state Markov process. The two states are: ON state representing occupied channel state and OFF state when the channel is idle. Both ON and OFF states temporal lengths are random variables (RV) with specific statistical distributions. ON and OFF temporal lengths are assigned the RVs x and y respectively throughout this thesis. The statistical distributions of x and y will be discussed in details with an empirical modeling in Section 4.2. Channel utilization factor or duty cycle, u, is defined as the ratio of time during which the channel is being utilized which is mathematically obtainable as

$$u = \frac{E\{x\}}{E\{x\} + E\{y\}}, \tag{2.3}$$

with $E\{\cdot\}$ denoting the expected value.

The SU locates and utilizes the spectrum opportunities by using the following model. The channel is sensed for a time t_s and in case of $\mathcal{H}_0$, the SU starts to transmit on the channel, otherwise, it senses another channel. The sensing is performed periodically with a period of T. The periodic sensing is done either to detect PU transmission reappearance on the channel or for proactive sensing purposes [61]. Moreover, in case of finding no free channel the sensing is resumed periodically too.

The opportunistic channel access is depicted in Fig 2.1. The ON states are represented by the higher level of the binary representation and the OFF states are represented by the lower state. Missed opportunities and mutual operation are described in Section 2.3.

2.3 Performance Metrics

In different parts of the thesis, for either evaluation or optimization concerns, different performance metrics are used. In this section these performance metrics are

described with their corresponding notation and mathematical formulation. Later, throughout different chapters and/or appended publications respective performance metrics used are more explained. The performance metrics are presented in two groups, the first group contains the metrics defined previously in the literature while the second group is the group of the performance metrics defined in the thesis. Following are the used pre-defined performance metrics in the literature.

1. **Conditional probability of false alarm, p_{fa}:** Is the conditional probability of wrongfully detecting a signal existence when noise only is present [54,55]. In the binary hypothesis framework, p_{fa} is formulated as

$$p_{fa} = Pr\left(\mathcal{H}_1|\mathcal{H}_0\right). \tag{2.4}$$

2. **Total probability of false alarm, $\bar{p}_{fa}$:** Is the probability of falling in false alarm through the whole time [54, 55]. Therefore, $\bar{p}_{fa}$ is obtained as

$$\bar{p}_{fa} = (1-u) \cdot Pr\left(\mathcal{H}_1|\mathcal{H}_0\right). \tag{2.5}$$

3. **Conditional probability of detection, p_d:** Is the conditional probability of truly detecting an existing signal [54,55]. Hence, p_d is statistically obtained as

$$p_d = Pr\left(\mathcal{H}_1|\mathcal{H}_1\right). \tag{2.6}$$

4. **Total probability of detection, $\bar{p}_d$:** Is the detection probability through the whole time which is found as [54, 55]

$$\bar{p}_d = u \cdot Pr\left(\mathcal{H}_1|\mathcal{H}_1\right). \tag{2.7}$$

5. **Receiver operating characteristics, ROC:** In most cases, the detectors are designed to achieve a specific pre-set value of either conditional probability of false alarm or conditional probability of detection and the other detector parameters are set accordingly. For example, if the conditional probability of false alarm is fixed, then the conditional probability of detection will change accordingly. The relations between the values of p_{fa} and p_d are found in form of curves called ROC curves [62].

6. **Sensing time, t_s:** Is the time required to collect the samples and perform the sensing. Sensing time is used as a measure for sensing complexity in this thesis

7. **Transmission efficiency, η:** Is the fraction of time during which a SU is utilizing a free channel between two sensing instances. Transmission efficiency is formulated assuming that SUs can perform one task at a time either sensing or transmitting. Hence, transmission efficiency is found as

$$\eta = \frac{T}{T + t_s}. \tag{2.8}$$

8. **Captured opportunities, ζ:** As the sensing is performed periodically in a discrete points in time, the following situation is experienced: The sensing declares an occupied channel, however, the channel state changes from ON to OFF state one or more times within a period of T. Meanwhile, the SU captures a fraction of opportunities, call it ζ and misses $(1-\zeta)$ of the opportunities on that channel. ζ is dependant on the distributions of the ON and OFF periods. In Chapter 4, more explanation on finding ζ is provided.

Below are the major performance metrics introduced and used in the thesis. Some other performance metrics will be introduced locally in different chapters and sections

1. **Probability of right detection, p_{rd}:** Is defined as the conditional probability of detecting the existing signals and having no false alarms. Therefore, p_{rd} is found as
$$p_{rd} = p_d(1 - p_{fa}). \tag{2.9}$$

2. **Spectrum utilization factor (SUF):** Is the fraction of available spectrum opportunities in the whole sharing system that SU can locate and utilize.

3. **Mutual operation (MO):** In contrast to the captured opportunities, if the sensing outcome is $\mathcal{H}_0$, the channel state can change from OFF to ON state once or more within a period of T while the SU is utilizing it. Therefore, during a fraction of T both the PU and SU mutually use the same channel. This fraction of time of MO is derived in Chapter 4.

4. **Sharing throughput drop, χ:** Is the ratio between the decrease in the SU throughput due to mutual operation or channels unavailability and the throughput if the SU takes the role of the PU and exclusively uses a specific channel. More elaboration on χ is provided in Chapter 4

2.4 Performance Evaluation Approaches

To evaluate a sensing technique, either synthetic data using simulations or empirical data from measurements is used. Moreover, both simulations and measurements can be used as complements to each other. This section describe the evaluation signals and the measurements setup.

Evaluation Signals

WCDMA-like signals are adopted for either Monte-Carlo simulations or measurements. WCDMA-like signals are defined as signals with similar statistical properties as WCDMA signals (i.e., colored Gaussian noise) but they are not generated in the same way as WCDMA signals. WCDMA are therefore band limited Gaussian signals inside their occupation bandwidth, b [63]. Besides, there exists Gaussian

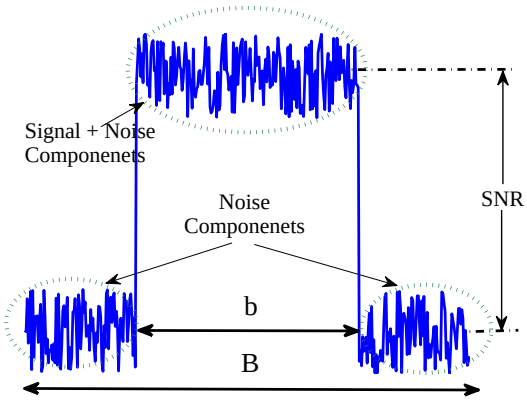

Figure 2.2: Spectra of the WCDMA-like evaluation signals.

noise that lies over the whole observation bandwidth, B. The ratio between the WCDMA-like signal variance and the noise variance represents the SNR. Fig. 2.2 depicts an example of the power spectral density (PSD) for a WCDMA-like signal used for simulations and measurements.

Measurements

Different measurements were carried out in the thesis for different purposes. Experimental validation together with simulations are used in functionality testing, performance evaluation and comparison in **Paper I**, **Paper II**, **Paper VII** and **Paper X**. Moreover, in **Paper V**, measurements were conducted for channel occupancy empirical modeling. Furthermore, real life communication signals including terrestrial TV signals and wireless microphone signals are captured for sensing purposes in **Paper IV**. Even though, different measurements were performed, yet, a generalized measurement setup is introduced in Fig. 2.3. The setup is divided into three units, namely, signal source unit, data capturing unit and control and data collection unit. Below are the descriptions for the three units.

Signal Source Unit

This unit represents the origin of the signal used later in the analysis. Four different sources are used in different studies. The first source is a vector signal generator (SG) which can produce either signals belong to different communication standards or loaded signals from a connected computer. In all measurements that used SG in the thesis, WCDMA-like signals are loaded from a PC into the SG. SG has been used in the measurement reported in **Paper I**, **Paper II**, **Paper VII** and **Paper X**. The second source is a wireless microphone transmitter placed close to a PC

repeatedly plays an audio signal to generate a frequency modulated (FM) wireless microphone signal. The SG and wireless microphone transmitter are the sources of the active laboratory measurements where signal sources are controlled throughout the measurements. The third signal source is a terrestrial TV transmitter. Both second and third sources are used in **Paper IX**. The fourth source is a cellular base station used in **Paper V** for PU traffic modeling. The measurements used the third and fourth sources are passive field measurements where no control over the signal sources takes place.

Data Capturing Unit

The measurements data is captured using one of three possible setups. The first setup is a spectrum analyzer (SA) connected directly to the SG, in this setup no wireless transmission takes place which is used in **Paper I**, **Paper II**, **Paper VII** and **Paper X**. The second setup is a receiving antenna connected to an SA where the radio signals coming from the wireless microphone or the terrestrial TV transmitter are obtained for the studies in **Paper IX**. The SA is connected to an external attenuator which is used together with the SA internal attenuation to adjust the SNR. The third data capturing setup is a receiving antenna feeding a real time spectrum analyzer (RTSA) to collect real time data for channel occupancy modeling performed in **Paper V**.

Control and Data Collection Unit

The measurements campaigns are automatized using the control and data collection unit which is a PC running MATLAB connected to the SG, SA and RTSA and controls their parameters. Moreover, the PC records the data captured by either the SA or RTSA for further analysis.

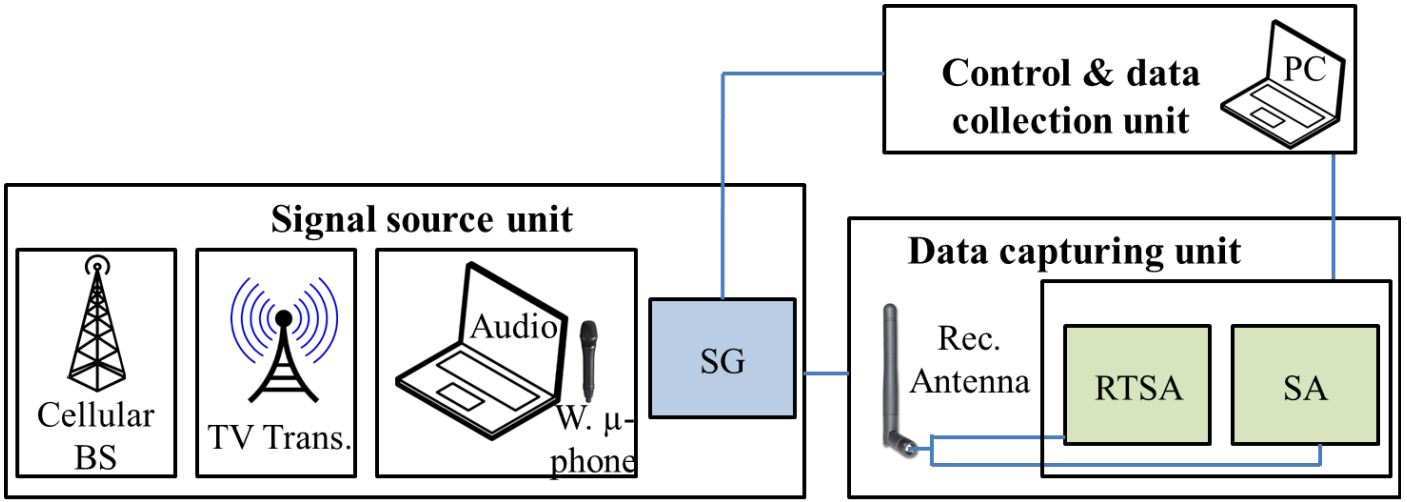

Figure 2.3: Measurement setup.
Cellular BS: Cellular base station. **TV Trans:** Terrestrial TV transmitting tower. **W.μ-phone:** Wireless micro-phone transmitter. **Rec. Antenna:** Receiving antenna. **SG:** Vector signal generator. **SA:** Spectrum analyzer. **RTSA:** Real time spectrum analyzer. **PC:** Personal computer.

Chapter 3

Studied Blind Sensing Techniques

THREE techniques are involved in the studies carried out in this thesis, namely, energy detector (ED), maximum-minimum eigenvalue detector (MME) and spectrum discriminator (SD). ED and MME are existing techniques used in different studies throughout the thesis. In contrast, SD is a sensing technique developed as a stand-alone contribution of this thesis.

ED and MME parameters are optimized to achieve as reliable as possible performance reflected by the performance metrics illustrated in Section 2.3. The optimizations carried out for both ED and MME are covered in Chapter 4. Furthermore, after optimizing the performance of both ED and MME, a fully-blind self-adapted two stage detector composed of ED and MME is designed. Therefore, ED and MME are considered as *row materials* of most of the thesis contributions.

ED, MME processes are presented in brief in this chapter. Moreover, this chapter introduces the SD and provides a comparative study of SD, ED and MME. Thereafter, using the SD for peeling off different PUs as a wideband sensing technique is explained in this chapter. This chapter summarizes the contributions included in **Paper I** and **paper II**.

3.1 Energy Detection

Energy detection is the process of calculating the energy of a received signal inside a specific band and comparing it with the noise energy presents in that band. Suppose the signal energy is calculated from N samples, single vector received signal (i.e. $L = 1$ in (2.2). Hence, x_j, s_j and z_j will be used to denote the j^{th} sample in the received signal bearing noise, signal and noise only components respectively. In ED, the decision is taken as

$$\mathbf{X} \rightarrow \begin{cases} \left(\sum_{j=1}^{N} |x_j|^2\right) < \rho & \mathcal{H}_0 \\ \text{Otherwise} & \mathcal{H}_1 \end{cases}, \tag{3.1}$$

where ρ is the detection threshold and the way to determine it is described in the following part of this section. The output of the ED is Chi-square distributed which can be approximated as a Gaussian distribution under the assumption of $N \to \infty$ [54, 55]. Based on this approximation, the conditional probability of false alarm for the ED, p_f^E, is obtained as

$$p_f^E = Q\left(\frac{\rho - N\sigma_z^2}{2\sqrt{2N}\sigma_z^2}\right), \tag{3.2}$$

where $Q(\cdot)$ is the Q function representing the complementary cumulative distribution function (CCDF) of a Gaussian random process and σ_z^2 is the noise variance. If the probability of false alarm for the ED is pre-set and the other parameters are calculated accordingly, then, from (3.2) the detection threshold, ρ, is determined as

$$\rho = \sqrt{2N}\sigma_z^2 Q^{-1}(p_f^E) + N\sigma_z^2, \tag{3.3}$$

where $Q^{-1}(\cdot)$ is the inverse Q function. After obtaining the value of ρ, the probability of detection of the ED, p_d^E, is calculated using

$$p_d^E = Q\left(\frac{\rho - N(\gamma_0 + 1)\sigma_z^2}{2\sqrt{2N}(\gamma_0 + 1)\sigma_z^2}\right), \tag{3.4}$$

with γ_0 denoting the received SNR.

3.2 Maximum-Minimum Eigenvalue Detection

Random matrix theory (RMT) in general and covariance matrix eigenvalues distribution in particular have been widely used in solving wireless communication related problems [64, 65]. MME is one of the algorithms that employ the covariance matrix eigenvalues distribution to perform spectrum sensing. This section presents the essence of the MME detector introduced in [39, 40]. Starting from the assumption of having a zero mean, σ_z^2 variance white Gaussian noise, when N and $L \to \infty$ then the noise statistical covariance matrix $\mathbf{R}_z$ is defined as

$$\mathbf{R}_z = E\{\mathbf{Z}\mathbf{Z}^H\} = \sigma_z^2 \mathbf{I}_L, \tag{3.5}$$

where $(\cdot)^H$ denotes the complex conjugate and $\mathbf{I}_L$ is the identity matrix of order L. In the same way, the statistical covariance matrices of $\mathbf{X}$ and $\mathbf{S}$ are $\mathbf{R}_x$ and $\mathbf{R}_s$ respectively and they are defined as $\mathbf{R}_x = E\{\mathbf{X}\mathbf{X}^H\}$ and $\mathbf{R}_s = E\{\mathbf{S}\mathbf{S}^H\}$. Since the signal and noise are independent, then $\mathbf{R}_z$ is expressible as

$$\mathbf{R}_x = \mathbf{R}_s + \sigma_z^2 \mathbf{I}_L. \tag{3.6}$$

As there exists a finite number of samples, the *sample* covariance matrices (SCM) is computed instead of the statistical covariance matrices. The SCM of the received signal is obtained as

$$\hat{\mathbf{R}}_x = \frac{1}{N}\mathbf{X}\mathbf{X}^H. \tag{3.7}$$

Now suppose that $\hat{\mathbf{R}}_x$ has the descending ordered eigenvalues $\lambda_1, \lambda_2, ...\lambda_L$. Similarly, the SCM of the signal $\hat{\mathbf{R}}_s$ has the descending ordered eigenvalues $\lambda_1^s, \lambda_1^s, ...\lambda_1^s$. Also the noise SCM descending ordered eigenvalues are $\lambda_1^z, \lambda_1^z, ...\lambda_1^z$. Accordingly,

$$\lambda_n = \lambda_n^s + \lambda_n^z, 1 \leq n \leq L. \tag{3.8}$$

Under the condition of signal absence, $\mathbf{X} = \mathbf{Z}$ is a zero mean Gaussian random variable and $\hat{\mathbf{R}}_x$ is a Wishart matrix. Therefore, the maximum eigenvalue of $\hat{\mathbf{R}}_x$ has a probability density function (PDF) that follows Tracy-Widom distribution of order 1 [39, 40, 66, 67]. From this background, to declare a signal existence or absence, a detection threshold, Λ, of the ratio between the maximum and the minimum eigenvalue, λ_1 and λ_L, is set. The probability of false alarm, p_f^M as a function of Λ is derived in [39] as

$$p_f^M = 1 - F_1 \left(\frac{\Lambda \left(\sqrt{N} - \sqrt{L}\right)^2 - \left(\sqrt{N} + \sqrt{L}\right)^2}{\left(\sqrt{N} + \sqrt{L}\right)^2 \left(\frac{1}{\sqrt{N}} + \frac{1}{\sqrt{L}}\right)^{\frac{1}{3}}} \right), \tag{3.9}$$

where $F_1(\cdot)$ is the Tracy-Widom distribution of order 1. If the MME is set to achieve a specific probability of false alarm, then Λ is calculated as

$$\Lambda = \left(\frac{\sqrt{N} + \sqrt{L}}{\sqrt{N} - \sqrt{L}} \right)^2 \left(1 + \frac{(\sqrt{N} + \sqrt{L})^{-2/3}}{(NL)^{1/6}} F_1^{-1}(1 - p_f^M) \right), \tag{3.10}$$

where $F_1^{-1}(\cdot)$ is the inverse of the Tracy-Widom distribution of order 1. In the context of binary hypothesis testing, MME obtains the maximum and minimum eigenvalue of the received signal SCM and then performs the detection as

$$\mathbf{X} \rightarrow \begin{cases} \left(\frac{\lambda_1}{\lambda_L}\right) \leq \Lambda & \mathcal{H}_0 \\ \text{Otherwise} & \mathcal{H}_1 \end{cases}. \tag{3.11}$$

3.3 Spectrum Discriminator

Performing blind spectrum sensing is motivated by PU signal and noise information unavailability in practice. However, blind spectrum sensing algorithms developed in the literature are in general computationally expensive [39–46, 48–51]. Therefore, developing a computational efficient blind sensing technique is a need which is provided in **Paper I** and **Paper II** and called spectrum discriminator (SD). SD uses discriminant analysis statistical framework to perform sensing.

The main philosophy of discriminant analysis is to partition a data into two groups such that the groups means are maximally separated under the constraint

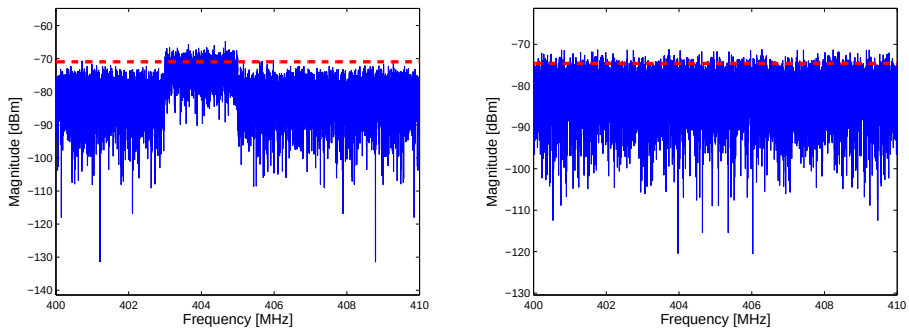

(a) (b)

Figure 3.1: Discrimination height (red dashed line) for: a) 10 dB SNR received signal and b) Noise only signal.

that the variance within every group is as small as possible. Discriminant analysis is performed by maximizing the test statistic $\mathcal{T}^2$ which is found as

$$\mathcal{T}^2 = \frac{\hat{A}_z^I - \hat{A}_z^J}{\hat{\sigma}_I^2(I-1) + \hat{\sigma}_J^2(J-1)}(I+J-2). \tag{3.12}$$

The relation in (3.12) is called Fisher's quadratic discriminant [68], in which $\hat{A}_z^I$ represents the mean amplitude of the spectral lines classified as signal. $\hat{A}_z^J$ represents the mean amplitude of the classified noise lines. The variables I and J represent the respective number of classified signal and noise lines. Finally, $\hat{\sigma}_I^2$ and $\hat{\sigma}_J^2$ are the respective variances of the amplitudes of the classified signal and noise lines. Since the objective of the discriminant analysis is to maximize (3.12), therefore, the set of frequency bins of the signal lines I and of the noise lines J should be chosen in such a way that the numerator or distance between the group means is maximized, and the denominator or distance within the group variances is minimized. A binary grid search is used to come to the correct border between the two groups referred to as the discrimination height.

Fig. 3.1a illustrates the discrimination height for a spectrum containing noise and 10 dB SNR signal. After specifying the discrimination height, the average energy inside the band of interest can be calculated. If this calculated average energy exceeds the average energy of the spectral lines in the noise group (i.e. the lower group) one assumes that a PU signal is present. A problem arises when noise only (i.e., no signal) is applied to the test statistic. Since the noise is not absolutely flat, a discrimination height will still be selected and two groups will still be discriminated as depicted in Fig. 3.1b. Two solution to overcome this limitation are proposed as explained below.

The first proposed solution is to set a noise uncertainty value, δ, which reflects the range over which the noise energy can vary. Hence, it is assumed that the noise

energy is $\hat{A}_z^J \pm \frac{\delta}{2}$. Since we are interested in the upper bound of the noise energy upon our pre-set value of δ, then the detection threshold is $\hat{A}_z^I + \frac{\delta}{2}$. If the band to be sensed consists of spectral lines having indices between f_l and f_h, then the detector performs the binary hypothesis testing as

$$r(t) \rightarrow \begin{cases} \frac{1}{(f_h - f_l)} \sum_{k=f_l}^{f_h} A_z(k) \leq \left(\hat{A}_z^I + \frac{\delta}{2} \right) & \mathcal{H}_0 \\ \text{Otherwise} & \mathcal{H}_1 \end{cases} . \tag{3.13}$$

As an alternative to the noise uncertainty approach, a probabilistic validation approach can also be used to perform the detection. With the probabilistic validation, the classified signal lines are fitted to a Rician distribution while the noise only lines are fitted to a Rayleigh distribution as the noise components are circular Gaussian distributed [69]. Following that, the signal lines with higher probability of falling in the Rayleigh distribution than in the Rician distribution are considered to be misclassified. Subsequently, those lines are reclassified as noise only components and hard decision among all the lines is performed.

3.4 Comparative Study among ED, MME and SD

The performance of SD has been compared with the performance of ED and MME. The comparison concerns the probability of false alarm, p_{fa}, and the probability of detection, p_d. Following are the analysis of the results of the probability of detection.

From Fig. 3.2 it can be observed that for spectrum discriminator, increasing the noise uncertainty δ decreases the detector performance in terms of the probability of detection, p_d. This trend is due to the fact that more signals will be detected as noise when the noise energy margin becomes wider. For the MME, Fig. 3.2 shows that increasing either the number of collected samples, N, or the number of vectors, L, would increase the probability of detection p_d. We can conclude that the probability of detection p_d of the SD is very much dependant on the noise uncertainty value, δ and it outperforms the MME and ED for all simulated parameters when $\delta = 0$ dB.

The findings of the probability of detection have to be compromised by the corresponding probabilities of false alarm and sensing times shown in Fig. 3.3 and Table 3.1, respectively. Generally, The choice between using SD, ED and MME with different parameters depends on the requirements of the application in order to obtain the most appropriate trade off between the probability of detection, the probability of false alarm and the sensing complexity.

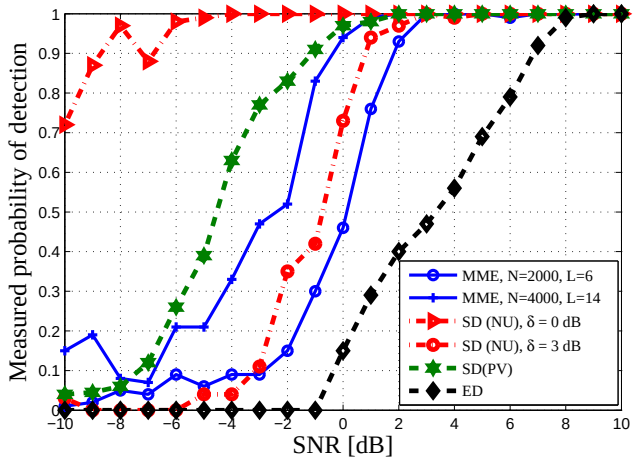

Figure 3.2: Results for the probability of detection for SD, MME and ED. NU: noise uncertainty. PV: probabilistic validation.

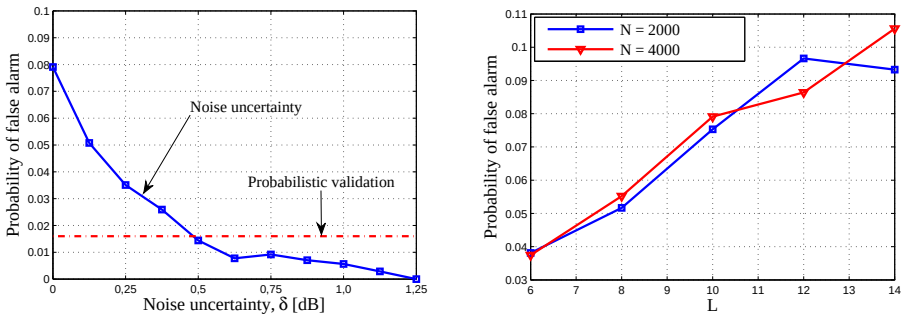

(a) (b)

Figure 3.3: Results for the probability of false alarm for a) SD. b) MME.

Table 3.1: Simulation results for sensing time for SD, ED and MME.

Sensing technique and parameters	Sensing time [sec]
SD (NU)	3.3
SD (PV)	6.5
ED	1.1
MME	7.1 - 27.6 [a]

[a] sensing time for MME highly depends on N and L which have been changed in a wide range.

3.5 Peeling off PUs using SD

Assume that the sensed spectrum using SD contains multiple PUs with a big difference between the SNRs of the strongest and the weakest PU. The spectrum discriminator will then consider the weakest PU as noise and will no longer be able to detect it. This is due to that discriminant analysis partitions the spectral lines into two groups only. Either the data falls in the noise group or in the signal group. As a result, the weak PUs signals fall wrongfully in the noise group. In this section, the discriminant analysis method is extended to a peel off technique that allows detecting all PUs based on an iterative algorithm.

The probability of misclassifying a noise line as a signal line denoted as $p_{mc}(k)$ is defined as

$$p_{mc}(k) = p(A_*(k) > A_x(k)|k \notin I). \tag{3.14}$$

When analyzing this probability of misclassification for every line, one will see that as expected the spectral lines belong to PUs present in the spectrum will have a low probability of misclassification. Based on this observation an iterative algorithm is developed as follows.

A set of the spectral lines injected to the SD is defined as $\mathcal{X}$. At first $\mathcal{X}$ contains all the spectral lines in the whole band. In each iteration, the values of $p_{mc}(k)$ for the spectral lines in $\mathcal{X}$ are computed. Those lines for which $p_{mc}(k) < \phi$ are considered to be PU signal lines and excluded from $\mathcal{X}$. ϕ is a user-defined threshold that sets the sensitivity of the detection method. The larger the ϕ, the higher the probability that noise lines are wrongly classified as signal, and hence the higher the probability of false alarm. On the other hand, if the threshold ϕ is too small then the algorithm will no longer be able to detect very weak SNRs signals. The iterative algorithm is stopped when no lines are left over that satisfy the condition $p_{mc}(k) < \phi$.

To evaluate the performance of the peeling-off technique, two signals have been placed in the sensed spectrum. The first signal has a fixed SNR of 10 dB while the second signal SNR has been stepped from 0 to 10 dB with a step of 1 dB. The probability of detection, p_d, for the second (i.e., weaker) signal is evaluated by peeling off the PUs using different values of ϕ. The results in Fig. 3.4a show that the probability of detection, p_d, for the weaker signal increases when the value of ϕ increases. However, increasing ϕ would increase the probability of false alarm, p_{fa}, as depicted in Fig. 3.4b.

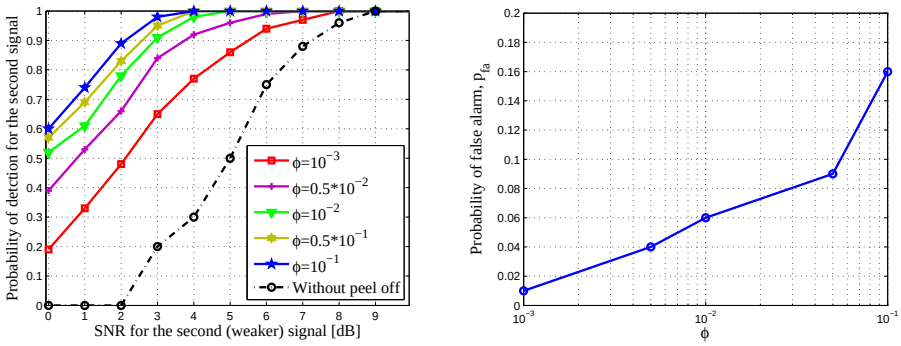

(a) (b)

Figure 3.4: Peeling off using different values of ϕ a) Probability of detection. b) Probability of false alarm.

Chapter 4

Sensing Performance Optimization

AS pointed out in Chapter 1, sensing optimization is one of the challenges faced by spectrum sensing. Different sensing techniques perform differently according to the used parameters. Accordingly, these parameters can be objectively optimized. In this chapter, optimizations of sensing parameters for ED and MME considering different objectives are carried out.

4.1 Optimization of Periodic Sensing using ED

In ED, the sensing time influences the detector performance in terms of the probability of false alarm and the probability of detection. Moreover, when periodic sensing is adopted, the periodic sensing interval affects the ability of the detector to grasp the spectrum opportunities and the ability of utilizing those opportunities. If we consider optimizing the sensing time and the periodic sensing interval for each channel in the PU spectrum, then the objective would be achieving as high detector performance and opportunities utilization in that channel as possible.

For a multi channel system, this objective will still hold with a different interpretation for opportunities utilization where it reflects the utilization for the whole available opportunities in all channels instead of each channel individually. In this context, one may optimize the sensing time or the periodic sensing interval for a single channel or a multi channel system, besides, both can be mutually optimized in both cases.

This section discusses two contributions related to sensing time and periodic sensing interval(s) optimization. At first, how to mutually optimize the sensing time and periodic sensing interval for an ED. Secondly, optimization of the periodic sensing intervals in a multi channel system is investigated.

Single Channel Scenario

In this investigation which is completely included in **Paper III** , a new approach to mutually optimize the sensing time and the periodic sensing interval for ED is proposed. The optimization of the sensing time objective is maximization of the summation of the probability of right detection, p_{rd}, and the transmission efficiency, η. On the other hand, the optimization of periodic sensing interval is subjected to maximizing the summation of the transmission efficiency and the captured opportunities.

The optimal sensing time referred to as t_s^* is obtained by maximizing the average of η and p_{rd} as

$$t_s^* = \arg\max_{t_s} \{0.5(\eta + p_{rd})\}. \tag{4.1}$$

For the periodic sensing interval, T, consideration, increasing T would increase the transmission efficiency, η, however, it would decrease the captured opportunities, ζ, and vice versa. Therefore, the optimal value of T, call it T^*, is reached by maximizing the average of η and ζ as

$$T^* = \arg\max_{T} \{0.5(\eta + \zeta)\}. \tag{4.2}$$

From (4.1) and (4.2), it is noticeable that both t_s^* and T^* are influenced by η which itself depends on t_s and T. Thus, in order to solve this optimization problem, an iterative calculation of t_s^* and T^* is proposed. The iterative mutual solution starts from an arbitrary value for either t_s or T and stop when they converge. To test the iterative mutual optimization algorithm, simulations are performed assuming that the PU channel ON and OFF periods are exponentially distributed with perfectly estimated means, μ_x and μ_y.

Figure. 4.1a shows the values of t_s obtained at each iteration for different values of μ_x and μ_y, starting from an arbitrary value of 10 ms for t_s. Similar to Figure 4.1a, Fig. 4.1b shows the values of T obtained iteratively for different values of μ_x and μ_y. For better visibility Fig. 4.1b is split into two sub-figures due to the big differences in the values of T^* when channel parameters change. As a general trend shown by Fig. 4.1, both t_s^* and T^* increase when the channel utilization factor, u, increases.

Periodic Sensing Optimization in a Multi Channel Scenario

In **Paper III** the sensing time and the periodic sensing interval have been optimized for a single channel. For the periodic sensing interval the optimization is done in order to maximize the summation of the captured opportunities, ζ, and the transmission efficiency, η. In **Paper IV** a multi channel system is considered for optimizing the periodic sensing interval for each channel. In a multi channel system, we assume that one channel is sensed at a time. The optimization of the periodic sensing intervals for the different channels can be done concerning maximizing the captured opportunities and the transmission efficiency for the whole

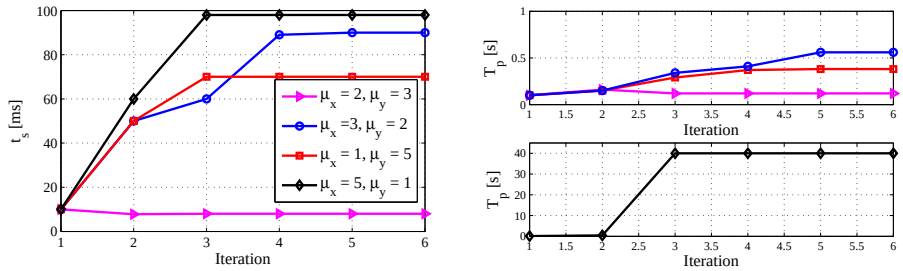

(a) (b)

Figure 4.1: a) Obtained optimal sensing times, t_s^*, with the iterations. b) Obtained optimal periodic sensing intervals T^* with the iterations.

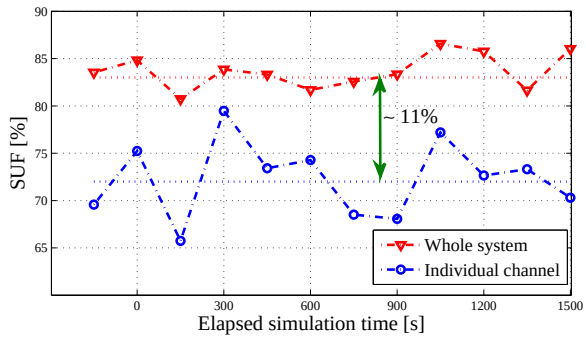

Figure 4.2: SUF with the consideration of whole system and individual channels utilization in optimizing periodic sensing intervals.

system. Consequently, for a multi channel system, the definition of the transmission efficiency is modified to consider the time spent on sensing other channels while communicating. Therefore, for a system with N_c channels, the optimum periodic sensing intervals vector, $\vec{T}^*$, is optimized as

$$\vec{T}^* = \arg\min_{T} \left\{ \sum_{i=1}^{N_c} (\eta_i + \zeta_i) \right\}, \tag{4.3}$$

where η_i and ζ_i are the transmission efficiency and the captured opportunities in channel i respectively.

Fig. 4.2 exhibits the attained spectrum utilization factor (SUF) (defined in Section 2.3) when individual channels' periodic sensing intervals are optimized independently and when the whole system is considered as in (4.3). According to the figure, average achieved SUF when optimizing the periodic sensing intervals

concerning the whole system outperforms the average SUF when each channel is treated independently by $\simeq 11\%$. Moreover, more consistent SUF is obtainable with the whole system consideration.

4.2 Empirical Channel Usage Modeling

This part of the thesis contribution, which is included in **Paper V**, is mainly exploring fitting the empirical data for the LTE channel occupancy into a mixture of exponential distributions combined linearly. Using distributions mixture is motivated by keeping the advantageous of the ease of exponential distributions in finding analytical solutions for the optimization problems (see Section 1.5). Moreover, distribution mixtures are more general than single distributions and can be used to fit the data under different conditions. Consequently, the algorithms developed based on exponential distributions as in Section 4.1 can still be used with a modification of considering the linear combination of multiple exponential distributions.

In [70] a linear combination of exponential pdfs is introduced to fit a heavy tail distributed data. For exponential mixture distribution, the pdf of a random variable θ is expressed as

$$f(\theta) = \sum_{i=1}^{k} w_i \cdot \frac{1}{\mu_i} e^{-\frac{1}{\mu_i}\theta}, \tag{4.4}$$

where k is the number of the distributions linearly combined, w_i is a weighting parameter satisfying $\sum_{i=1}^{k} w_i = 1$ and μ_i is the mean of the distribution i.

Assuming that $\mu_i > \mu_{i+1}$, then there is a region in the distribution tail that can be exclusively fit with $w_1 \cdot 1/\mu_1 e^{-1/\mu_1\theta}$. Moreover, there is a preceding region that can be fit with $(w_1 \cdot 1/\mu_1 e^{-1/\mu_1\theta} + w_2 \cdot 1/\mu_2 e^{-1/\mu_2\theta})$ and so on. Accordingly, finding w_i and μ_i can be done as a recursive procedure starts with fitting the tail and moving backwards. Fig. 4.3 illustrates the idea of the exponentials mixture recursive fitting procedure. The full explanation on the recursive procedure is found in [70].

The empirical downlink LTE traffic is obtained through a measurement campaign performed in Kista, Stockholm, Sweden. The measurement setup is depicted in Fig. 2.3 with an LTE base station acting as the signal source unit and an antenna connected to an RTSA acting as the data capturing unit. Since different channels experience different loads at different times, the measurements are treated in time spans of 2 hours. Below is a representative case of the results. This representative results are for the measurements carried out for a 1.4 MHz channel lies between 2650.6 and 2652.0 MHz during the period: Wednesday, October, 02, 2013, 09:00 am to 11:00 am. Fig. 4.4 shows the empirical distribution and the fitted exponential distributions mixtures. The figure shows how the fitted mixture approaches towards the empirical distribution with the change of k.

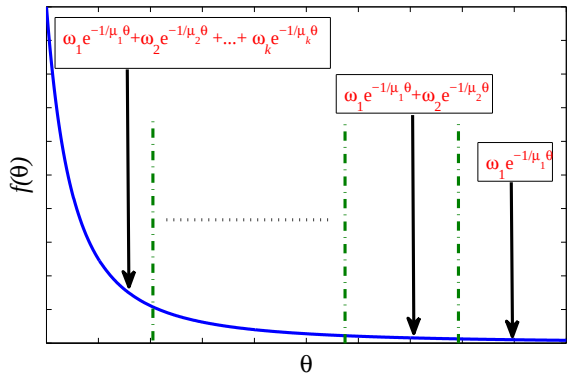

Figure 4.3: Illustration of exponential distributions mixture fitting methodology.

As it is shown in Fig. 4.4, the lower values of k make the exponential mixture to fit the tail with poor fitting for the lower values of x. In contrast, increasing k improves fitting the lower region of x. This is explained as follows; as the first pair (w_1, μ_1) always characterizes the heaviest part of the distribution tail, then there is always a guarantee that all the values in that heaviest part are well fitted, depending on the obtained values of (w_1, μ_1) and the value of k, rest pairs (w_i, μ_i) are obtained and the last pair (w_k, μ_k) is fully dependant on the previous obtained pairs. Therefore, when k increases the part that is characterized by (w_k, μ_k) decreases.

A quantitative evaluation of the fitted distribution is obtained by means of the log likelihood estimation which is defined as [71]

$$\Phi(\theta|g(\theta)) = \int f(\theta)\log\left(\frac{g(\theta)}{f(\theta)}\right) d\theta, \tag{4.5}$$

where $\Phi(\theta|f(\theta))$ is the log-likelihood estimation for a random variable θ having an empirical pdf $f(\theta)$ and fitted to a distribution with a pdf $g(\theta)$. Table 4.1 shows the log-likelihood estimation for different distributions. The log-likelihood estimation is calculated for fitting both x and y in the same period as the one used to generate Fig.4.4.

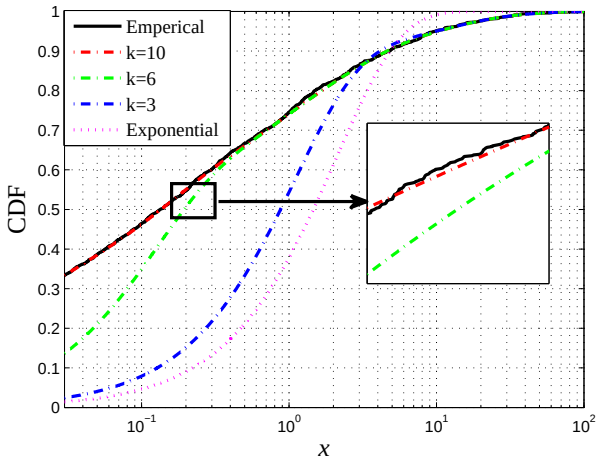

Figure 4.4: The empirical and fitted CDF for exponential distributions mixture with different values of k.

Table 4.1: Log-likelihood for fitting different distributions. The fitted date is for the ON lengths, x, and the OFF lengths, y in the period Tuesday, October , 01, 2013, 12:00 - 16:00.

Distribution		$\Phi(x\|f(x))$	$\Phi(y\|f(y))$
Exponential		0.368	0.377
Lognormal		0.017	0.013
Generalized Pareto		0.032	0.029
Exponentials mixture	$k=2$	0.292	0.244
	$k=3$	0.220	0.228
	$k=4$	0.136	0.131
	$k=5$	0.068	0.066
	$k=6$	0.064	0.063
	$k=7$	0.020	0.019
	$k=8$	**0.005**	**0.004**

4.3 Sensing Optimization in LTE Cognitive Femto-cells

In the context of handling the demands of higher data rates in mobile networks, network operators are approaching towards more distributed networks architecture. In

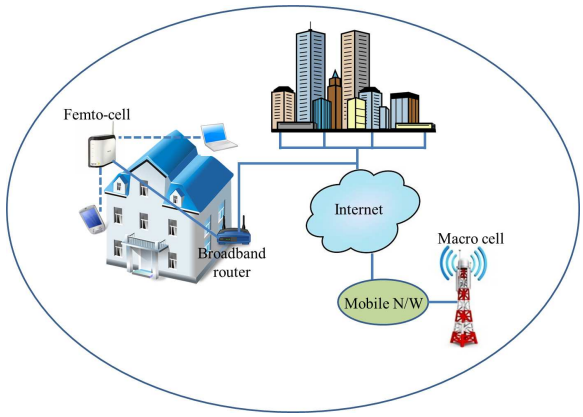

Figure 4.5: Two-tier heterogeneous cellular network.

this regard, the third generation partnership project (3GPP) framework standards support deployment of low power reduced scale plug and play access points known as femto-cells [72]. Femto-cells are attached to the mobile core network through the internet cloud. The network composed of macro-cells which offload portion of their traffic into femto-cells is called two-tier heterogeneous cellular network as shown in Fig. 4.5.

From radio resources prospective, femto-cells can use the same radio spectrum assigned for the macro-cell base station (MBS). In this case, MBS and femto-cells share the spectrum under DSA framework where MBSs act as PUs and femto-cells with CR capabilities called cognitive femto-cells base stations (FBS) take the role of SUs. Consequently, higher network throughput is achieved using the same licensed spectrum owned by the network operator [73]. The reader is referred to [74–76] for more literature review on the potentials of FBS deployment.

In **Paper VI** periodic sensing intervals for ED are optimized in LTE two-tier network with the objective of maximizing the FBS throughput in a multi channel scenario. Energy detector is used to locate the free channels. Moreover, the findings of **Paper V** summarized in Section 4.2 are used as a representative of a real life channel occupancy statistical pattern.

Downlink Throughput Maximization Based Sensing

FBS are deployed to enhance the network throughput using the same spectrum assigned for the MBS. Hence, the periodic sensing is optimized with an objective of maximizing the FBS throughput as explained hereafter.

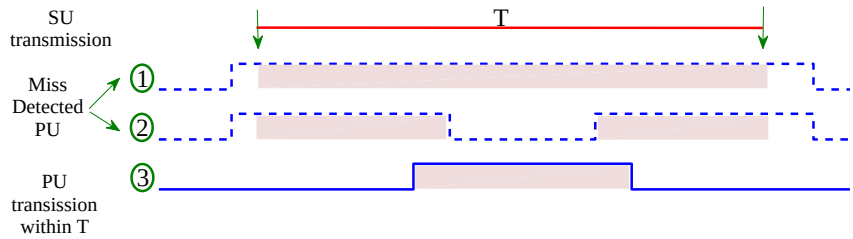

Figure 4.6: PU-SU mutual operation cases.

MBS-FBS Interference Model

With the low transmission power of the FBS compared to the MBS, the interference due to the mutual operation is assumed to be from the MBS to the FBS but not in the opposite direction. In general, with spectrum sensing, three cases of mutual operation can occur depending on the sensing outcome. These three cases are explained below

1. *Case 1*: An active PU for a time longer than T is miss-detected. Subsequently, the SU starts transmitting on the channel simultaneously with the PU.
2. *Case 2*: Same miss-detection takes place as in case 1. However, the activity of the PU changes within a period of T one or more times.
3. *Case 3*: In this case, the SU operates on a channel based on a correct detection of PU absence. However, after a time less than T, the PU resumes its transmission with or without changing its status thereafter.

Fig. 4.6 demonstrates graphically the three cases of mutual operation. For LTE FBS, the FBS shares the same spectrum used by the MBS serving the area where the FBS is deployed. Therefore, high MBS received SNR is expected which assures a robust detection. Accordingly, the probability of miss-detection is practically zero and therefore occurrences of cases 1 and 2 are neglectable. If τ is defined as the fraction of time during which MBS and FBS mutual operation is experienced due to case 3, and the OFF periods, y, are distributed as a mixture of exponential distributions, then τ is obtained as

$$\tau = (1 - p_{fa}) \left(1 - \sum_{i=1}^{k} w_i^y \mathrm{e}^{\frac{-1}{\mu_i^y} T} \right). \tag{4.6}$$

In order to calculate the interference during the mutual operation periods, the interfering power from the MBS is calculated using the outdoor-to-indoor (O-I)

LTE signal propagation model in [77]. where the path loss from the MBS to an indoor terminal, PL_M, is found by

$$PL_M = 36.7\log_{10}(R) + 26\log_{10}(f_c) + 0.5d + 42.7, \tag{4.7}$$

where R, d and f_c denote the distance between the MBS and the building containing the terminal, the indoor distance between the wall and the terminal and the operation frequency respectively. To count for the shadow fading the path gain is modeled as a zero-mean log-normal distributed RV with a standard deviation σ_M. In the same way, the path loss from the FBS to the terminal, PL_F, is calculated using the indoor LTE path loss model in [77] as

$$PL_F = 43.3\log_{10}(d) + 20\log_{10}(f_c) + 11.5. \tag{4.8}$$

Similar to the O-I propagation model, the indoor path gain is modeled as a log-normal zero-mean RV with a standard deviation σ_F.

Periodic Sensing Optimization

The FBS provides two classes of throughput; when it is transmitting in the interference free instances and when it experiences interfered transmission. The interference free transmission throughput denoted as C_0, is limited by the SNR, γ_0 as

$$C_0 = W\log_2(1+\gamma_0), \tag{4.9}$$

where W is the channel bandwidth. On the other hand, during the interfered transmissions periods, the throughput, C, is limited by the signal to interference plus noise ratio (SINR), γ, and is equivalent to

$$C = W\log_2(1+\gamma). \tag{4.10}$$

To compute the throughput during the whole operation time denoted as C_{all}, C_0 and C are weighted by $(1-\tau)$ and τ respectively and accumulated. Moreover, it should be noted that the FBS is efficiently transmitting with a factor of the transmission efficiency, η, during a fractional time equivalent to the captured opportunities [1]. In a multi channel system having N_c channels available for sharing, the captured opportunities for the whole system, call it ζ_s, is found as

$$\zeta_s = 1 - \prod_{i=1}^{N_c}(1-\zeta_i), \tag{4.11}$$

where ζ_i is the captured opportunities on channel i. Accordingly, C_{all} is expressible as

$$C_{all} = \eta\zeta_s\big[(1-\tau)C_0 + \tau C\big]. \tag{4.12}$$

[1]It is assumed that no transmission during sensing and no transmission takes place if no free channels are found.

From Section 2.3, the throughput drop χ is defined as the ratio between the drop in the expected throughput due to the opportunistic access and the interference free expected throughput. Mathematically, χ is obtained as

$$\chi = 1 - \frac{E\{C_{all}\}}{E\{C_0\}}. \tag{4.13}$$

χ is then calculated as a function of τ using

$$\chi = 1 - \eta\zeta_s \left(1 - \frac{\tau}{A}\right), \tag{4.14}$$

where A is a constant found as

$$A = \left(\frac{P_t^F - PL_F - \sigma_z^2}{P_t^M - PL_M - \sigma_z^2}\right),$$

with P_t^F and P_t^M denoting the equivalent isotropic radiated power (EIRP) of the FBS and MBS respectively. Minimizing the throughput drop, χ, gives the optimal solution for the periodic sensing intervals vector $\vec{T}^*$. Accordingly,

$$\vec{T}^* = \arg\min_{T} \left\{1 - \eta\zeta_s \left(1 - \frac{\tau}{A}\right)\right\}. \tag{4.15}$$

Key Results

The occupancy in a span of 40 MHz in the 2.6 GHz LTE band is measured. The measurements findings in terms of the modeled channel occupancy using exponential distributions mixture are used as an input for a simulation study. The simulation is carried out to evaluate the throughput based sensing optimization discussed in the preceding part of this section. The used simulation and model parameters are presented in Table 4.2 below.

For benchmarking purposes, senseless throughput, C_{SL}, is defined as the FBS senseless throughput when no sensing is performed [78]. Fig. 4.7 exhibits the senseless throughput in contrast to the optimal throughput achieved, C_{opt}, when sensing is adopted and optimized with an objective of maximizing the FBS throughput. Fig. 4.7 also shows the available interference free opportunities for FBS, $(1 - u)$, and the optimal throughput drop. All of the results shown in Fig. 4.7 are obtained using the measurements data taken in different periods of the day October, 02, 2013. This day has been randomly picked up. As shown by Fig. 4.7, the more the interference free opportunities, the higher the senseless throughput and the lower the optimal throughput drop. Therefore, with periodic sensing intervals optimization, the highest gain in the throughput is achieved with the lowest available opportunities. This result reflects the creditability of optimizing the periodic sensing intervals as the necessity of optimizing the throughput increases at the peaks of the traffic.

Table 4.2: Simulation and model parameters

Parameter	Value
Probability of false alarm, p_{fa}	1×10^{-3}
Sensing time, t_s	20 ms
MBS EIRP, P_t^M	40.0 dBm
FBS EIRP, P_t^F	23.85 dBm [a]
MBS - building distance, R	200 m
FBS - terminal distance, d	$5 - 10$ m [b]
log-normal standard deviation, σ_M	7 dB [77]
log-normal standard deviation, σ_F	4 dB [77]
Noise power, σ_z^2	-170 dBm/Hz
Number of channels N_c	2 channels
Combined exponential distributions k	8

[a] The value of P_t^F is adjusted to give an average interference free throughput of 100 Mbps.
[b] The value of P_t^F is adjusted to give an average interference free throughput of 100 Mbps.

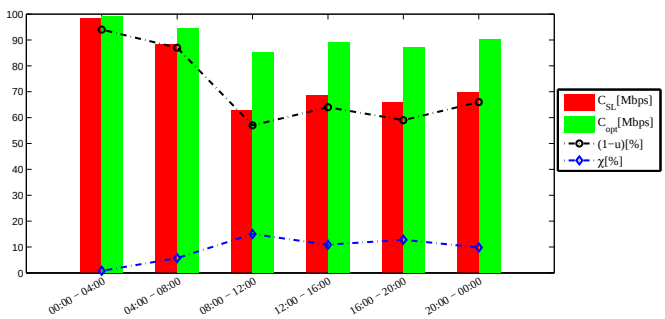

Figure 4.7: The senseless throughput, the optimal achieved throughput, the available opportunities for FBS and the minimum achieved throughput drop.

4.4 Performance Optimization of MME

Herein, MME performance is investigated and optimized considering two issues. Namely, filtering problem when using MME and signal bandwidth with respect to observation bandwidth. These two issues are both originated from the fact that MME requires an existence of noise only components when perform sensing. The filtering consideration tackles the problem of coloring the white noise when using

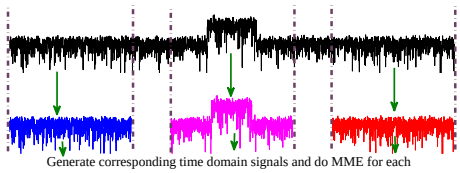

Figure 4.8: Illustration of sub-band spectrum scanning using FDRF. The spectrum of the whole band (black) is divided into three parts (blue, pink and red) each one represents one sub-band.

ordinary time domain filters. On the other hand, signal and observation bandwidth relation impact on detection accuracy is studied to find out how optimum detection is hit if adjusting observation bandwidth is doable, or, if not, then how the detection probability is mathematically formulated as a function of signal and observation bandwidths.

Frequency Domain Rectangular Filtering

With filtering, the spectrum of a received noise only components will be reshaped similarly to the filter transfer function. Therefore, the noise it is no longer Gaussian and MME can not be used.

To preserve the signal spectrum shape, a filter with a transfer function as in (4.16) is needed

$$H(f) = \begin{cases} 1 & f_l \leq f \leq f_h \\ 0 & \text{Otherwise} \end{cases}, \tag{4.16}$$

where f_l and f_h are the lower and upper frequency bounds of the band under sensing. To attain a transfer function as in (4.16), using of frequency domain rectangular filtering (FDRF) is proposed in **Paper VII** . FDRF preserves the signal frequency domain properties by slicing the spectrum into pieces, picking up the piece that represents the band under sensing, generate the corresponding time domain signal from that piece by means of the inverse Fourier transform and finally apply MME to the generated time domain signal. The remaining spectrum pieces are thrown away. Fig. 4.8 illustrates the idea of FDRF.

Bandwidth Impact on MME Detection

For MME detection, existence of noise only components is a necessary condition. Therefore, a question arises here is how the bandwidth of this noise only components would influence the MME detection performance. In this regard, the investigation in **Paper VIII** provides an analytical proof of the optimal signal and noise only bandwidths. The analytical proof is supported by simulations.

Gaussian Noise Covariance Matrix's Eigenvalues Distribution

The L eigenvalues of the of the $N \times L$ covariance matrix of a zero mean Gaussian process are distributed with a pdf follows Marchenko Pastur density function when N and $L \to \infty$ [79, 80]. If $L/N = c$, the variance of the Gaussian process is σ_z^2 and the L eigenvalues are assigned the RV ν then

$$f_\nu(\nu) = \frac{\sqrt{(\nu - \sigma_z^2(1-\sqrt{c})^2)\,(\sigma_z^2(1+\sqrt{c})^2 - \nu)}}{2\pi\sigma_z^2\nu c}, \tag{4.17}$$

with a support of

$$\sigma_z^2(1-\sqrt{c})^2 \leq \nu \leq \sigma_z^2(1+\sqrt{c})^2.$$

The density function shown in (4.17) is called Marchenko Pastur density function which is presented and proved in [81]. Hereafter, Marchenko Pastur density with the parameters c and σ^2 will be denoted as $\mathcal{MP}(c, \sigma_z^2)$.

Gaussian Signal Bearing Gaussian Noise Covariance Matrix's Eigenvalues Distribution

When a mixture of a signal occupying part of the observation bandwidth and a noise lies all over this observation bandwidth is received; then the samples covariance matrix, R_x, is not a Wishart matrix any longer and the distribution of its eigenvalues is unknown according to the best of our knowledge [39, 79, 80]. Therefore, finding a close form distribution for such scenario is a need which is one of the significant contributions of this thesis explained in the upcoming part of this section.

For the Gaussian signals, the occupation bandwidth contains a Gaussian process resulted from adding the Gaussian signal on top of the Gaussian noise, hence, the covariance matrix of the components inside the occupation bandwidth is a Wishart matrix. In addition to, the Gaussian noise has a Wishart covariance matrix. Therefore, the distribution of the eigenvalues of these two covariance matrices can be split into two Marchenko Pastur densities with different parameters as it is shown below.

Among the L eigenvalues of the mixture covariance matrix, there is l eigenvalues represent the signal on top of the noise and the rest $(L-l)$ are the noise only eigenvalues representatives. The quantity (l/L) will be denoted as β which is equivalent to the occupation/observation bandwidth ratio [79]. From (3.6), if the signal, $\mathbf{S}$, is a zero mean Gaussian inside the occupation bandwidth with a variance of σ_s^2 , then the following relation is valid

$$\mathbf{R}_x = \mathbf{\Psi}_{L,l} + \sigma_z^2\mathbf{I}_L, \tag{4.18}$$

where

$$\mathbf{\Psi}_{L,l} = \begin{pmatrix} \sigma_s^2\mathbf{I}_l & \mathbf{0}_{l,L-l} \\ \mathbf{0}_{L-l,l} & \mathbf{0}_{L-l,L-l} \end{pmatrix},$$

with $\mathbf{0}_{a_1,a_2}$ denoting a null matrix of size $a_1 \times a_2$. A reliable estimate of l called $\hat{l}$ is obtained using minimum descriptive length (MDL) criterion [82] as

$$\hat{l} = \underset{l}{\operatorname{argmin}} \left(-(L-l)N \log_{10} \left(\frac{\theta(l)}{\phi(l)} \right) + \frac{1}{2} l(2L-l) \log_{10} N \right), \tag{4.19}$$

where $\theta(l)$ and $\phi(l)$ are the geometric and arithmetic means of the smallest $(L-l)$ eigenvalues found by

$$\theta(l) = \prod_{i=l+1}^{L} \lambda_i^{1/(L-l)} \text{ and } \phi(l) = \frac{1}{L-l} \sum_{i=l+1}^{L} \lambda_i.$$

Consequently, $\hat{\beta}$ is estimated as $\hat{\beta} = \left(\hat{l}/L\right)$. Following that, the Marchenko Pastur density function corresponds to each group is found as

$$f_\nu(\nu) = \begin{cases} \mathcal{MP}\left(\hat{\beta}c, (\sigma_z^2 + \sigma_s^2)\right) & \lambda_l \leq \nu \leq \lambda_1 \\ \mathcal{MP}\left((1-\hat{\beta})c, \sigma_z^2\right) & \lambda_L \leq \nu \leq \lambda_{l+1} \end{cases}. \tag{4.20}$$

Optimum Observation/Occupation Bandwidth Ratio for MME: A proof

Below is an analytical derivation of the required observation/occupation bandwidth ratio for MME to achieve the highest sensing accuracy for a specific SNR. Assume that $\beta = 1$, then (4.18) turns out to be

$$\mathbf{R}_x = (\sigma_s^2 + \sigma_z^2)\mathbf{I}_L. \tag{4.21}$$

The covariance matrix at $\beta = 1$ takes the form in (4.21) due to that there are two independent zero mean Gaussian random series, the signal and the noise, added on top of each other. Consequently, the resultant output of this addition is a zero mean Gaussian random series with a variance of $(\sigma_s^2 + \sigma_z^2)$. Therefore, the null hypothesis, $\mathcal{H}_0$, will be declared when there is no signal or there exist a Gaussian signal occupying the whole observation bandwidth. In those two cases, the conditional probability of detection hits its minima which is the conditional probability of false alarm. Subsequently, the MME conditional probability of detection is a concave function of β and it has a maximum or maxima. Now if we move over to the covariance matrix domain, this conditional probability of detection curve maximum is reached when the probability of having a ratio of (λ_1/λ_L) greater than Λ is maximized.[2]

From (4.20), the eigenvalues correspond to both signal and noise components are bounded. Therefore, the maximum of (λ_1/λ_L) is reached when λ_1 reaches its

[2]Refer to Section 3.2 to revisit how MME performs the detection

upper bound and λ_L is at its lower bound. From (4.22) and (4.23) one can derive how (λ_1/λ_L) is related to β, c and γ_0 as

$$(\lambda_1/\lambda_L) = \frac{max\left\{\mathcal{MP}\left(\beta c, (\sigma_z^2+\sigma_s^2)\right)\right\}}{min\left\{\mathcal{MP}\left((1-\beta)c, \sigma_z^2\right)\right\}}. \tag{4.22}$$

This yields

$$\begin{aligned}(\lambda_1/\lambda_L) &= \frac{(\sigma_s^2+\sigma_z^2)\left(1+\sqrt{\beta c}\right)^2}{\sigma_z^2\left(1-\sqrt{(1-\beta)c}\right)^2}, \\ &= (1+\gamma_0)\left(\frac{1+\sqrt{\beta c}}{1-\sqrt{(1-\beta)c}}\right)^2, 0 \le \beta \le 1.\end{aligned} \tag{4.23}$$

Equalizing the derivative $\frac{d(\lambda_1/\lambda_L)}{d\beta}$ with zero will give a value of $\acute{\beta}$ as

$$\acute{\beta} = \frac{1}{2} \pm \frac{\sqrt{2c-c^2}}{2}. \tag{4.24}$$

Keeping in mind that the signal components are digitized to L portions when L eigenvalues of the received covariance matrix are computed. Hence, a single eigenvalue is representing $(1/L)$ of the signal components. Consequently, to have all the signal components represented by covariance matrix eigenvalues, $\acute{\beta}$ should be a multiple integer of $(1/L)$, call it β_{opt} which is found as

$$\beta_{opt} = \frac{1}{L}\left\lfloor \frac{L}{2}\left(1 \pm \sqrt{2c-c^2}\right)\right\rfloor, \tag{4.25}$$

where $\lfloor\cdot\rfloor$ denotes the closest smaller integer. In general, $N \gg 1$ which makes $c \ll 1$, Therefore, (4.25) is approximated as $\beta_{opt} \simeq 0.5$.

For simulation verification, WCDMA like signals having different SNRs and different occupation bandwidths. The generated WCDMA like signals are injected to an MME detector that uses $5000, 20,$ and 0.1 as values for $N, L,$ and p_f^M respectively. As Fig. 4.9 shows, the probability of detection for the detector, p_d^M, reaches its maximum value for each SNR when $\beta \simeq 0.5$ which verifies the previously shown analytical proof.

The occupation/observation bandwidth impact on MME performance exhibited in Fig. 4.9 can be applied in two types of systems differently as follows. For the systems such as terrestrial TV, in a specific geographical location, a number of channels are spread throughout the full broadcasting band. Therefore, the observation bandwidth is set as twice the channel bandwidth when detection is performed to achieve the optimal β. This setup is used under the assumption of having no two TV active adjacent channels in the same location. For other systems, such as cellular systems, the channels assignment is demand driven. Therefore, the guaranteed noise only portions are the guard bands. Hence, the curves in Fig. 4.9 are

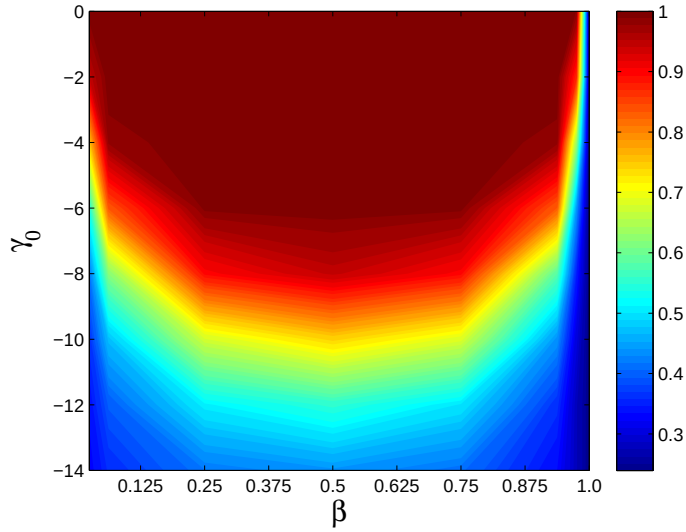

Figure 4.9: The probability of detection for MME for different values of observation/occupation bandwidth, β, and different values of the SNR, γ_0.

used to determine the achievable probability of detection at a specific received SNR considering the corresponding value of β.

Chapter 5

Blind Multi-stage Detection

WHEN comparing spectrum sensing techniques, the trade offs are mostly between the sensing accuracy and the complexity as depicted by Fig. 1.4. In general, more reliable detectors are more complex and consequently more costly in terms of hardware requirements and sensing time. Therefore, when the sensing is performed with no prior information about the received SNR, then going for an accurate and complicated technique is safe to assure the detection of low SNR signals [1]. However, performing complicated detection when the SNR is high is not needed when simple detection is capable. Hence, we can set an objective of gaining simplicity when high SNR signals are received and assuring reliable detection for the low received SNRs. This objective is not attainable using the same detector all the time, instead, one of two strategies can be employed. The first strategy is to switch among more than one detector connected in parallel depending on the received SNR which implies having SNR estimation phase assembled to the detection process [83–85]. The second alternative is to pass through a bank of detectors sequentially as explained in Section 5.1, this sequential approach is adopted in [86–88]. Both parallel and sequential approaches are referred to as multi-stahe spectrum sensing.

If blindness is considered together with the pre-mentioned objective, then when no information are available regarding the received signal, SNR estimation process adds more complication to the detection process. Therefore, sequentially connected detectors better perform blind detection concerning the simplicity-reliability objective.

In contrast to the state of the art in multi-stage spectrum sensing, **Paper IX** addresses the following missing points in the literature. At first, the literature seeks a generalized model for sequential multi-stage spectrum sensing which is developed in **Paper IX** and explained in this chapter. Secondly, a fully-blind, self-adapted

[1] The reliability here is reflected by the probability of detection dependency of the received SNR. It can also be seen as the value of the SNR wall of each technique [33]. Therefore, the lower the SNR wall, the more reliable the technique is.

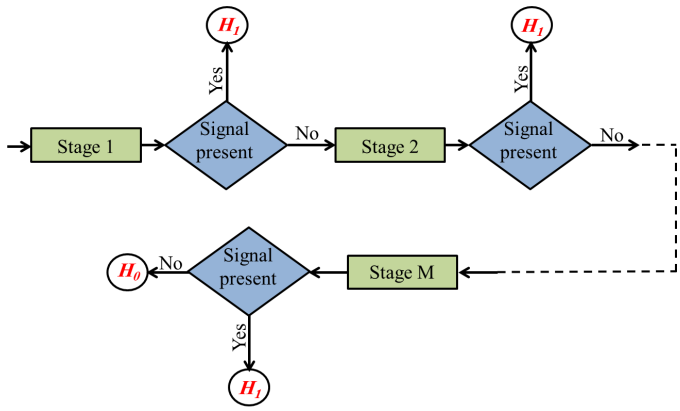

Figure 5.1: Sequential multi-stage spectrum sensing model.

multi-stage detector is proposed by using ED and MME. The explanation of the self-adaptability and full-blindness is provided in Sections 5.2 and 5.3. Moreover, with an exception to the SNR, influences of other signal parameters on detection performance are very limitedly studied. In this context, an investigation on the impact of the signal bandwidth inside the observation bandwidth on the detection performance of ED, MME and the proposed detector is carried out. This investigation employs and verifies the findings of **Paper VIII**. The proposed combined detector is tested with a measurement campaign for real-life signals.

5.1 Generalized Sequential Multi-stage Sensing Model

A generalized sequential multi-stage spectrum sensing model is proposed and explained in this section. The received signal is input to a bank of M detectors serially connected. Hereafter, this M bank detectors is denoted as M-stage detector. Let each stage to take an index i where $i = 1, 2, ..., M$ with $i = 1$ and $i = M$ representing the first and last stages respectively. Assume that the stage number i complexity is denoted as $\mathcal{C}^i$ and at a specific SNR, γ_0, it achieves a detection probability of $p_d^i(\gamma_0)$. Accordingly, the M detectors are placed from the simpler to the more complex which goes inversely with the reliability. This M-stages placement satisfies $p_d^1(\gamma) < p_d^2(\gamma) < ... < p_d^M(\gamma)$ and $\mathcal{C}^1 < \mathcal{C}^2 < ... < \mathcal{C}^M$.

The detection stops when $\mathcal{H}_1$ is declared at first. $\mathcal{H}_0$ is declared when all of the detection stages detect no signal. Therefore, the signals with high SNRs are detected in one of the early stages while the low SNR signals are required to pass through higher order stages. Fig. 5.1 depicts a schematic of the multi stage spectrum sensing. From the flow of the detection process in the sequential multi stage spectrum sensing shown in Fig. 5.1, the probability of detection for the whole

detector denoted as $p_d^{tot}(\gamma_0)$ is found as

$$p_d^{tot}(\gamma_0) = p_d^1(\gamma_0) + \sum_{i=2}^{M} \left(p_d^i(\gamma_0) \prod_{j=1}^{i-1} \left(1 - p_d^j(\gamma_0) \right) \right). \tag{5.1}$$

Similarly, if p_f^i is the i^{th} stage false alarm probability, then the probability of false alarm for the M stage detector is denoted as p_f^{tot} which is obtained by

$$p_f^{tot} = p_f^1 + \sum_{i=2}^{M} \left(p_f^i \prod_{j=1}^{i-1} \left(1 - p_f^j \right) \right). \tag{5.2}$$

The total complexity for the multi stage detector is obtained by summing up the individual complexities weighted by their usage. In the case of signal absence, each stage is used as long as no false alarm is introduce by one of its preceding stages. In the case of signal existence, each stage is used when the signal is miss detected by all of its preceding stages. Accordingly, the total complexity of the M stage detector, $\mathcal{C}^{tot}$, is derived as

$$\begin{aligned} \mathcal{C}^{tot} =& \mathcal{C}^1 + (1-u) \sum_{i=2}^{M} \prod_{j=1}^{i-1} \left(\mathcal{C}^i (1 - p_f^j) \right) \\ &+ u \cdot \sum_{i=2}^{M} \prod_{j=1}^{i-1} \left(\mathcal{C}^i \left(1 - p_d^j(\gamma) \right) \right), \end{aligned} \tag{5.3}$$

where u is the channel utilization factor explained in Chapter 2.

5.2 ED-MME Fully Blind Detector

As a specific case of multi stage detection, a two stage combined detector composed of ED and MME is developed. The developed detector is called **2EMC** standing for **2**-stages **E**D-**M**ME **C**ombined detector. Choosing ED and MME is motivated as follows. ED is used as a first stage detection for its simplicity which is the main concern in the first stage. MME is used as a second stage for two purposes. At first, MME can perform blind spectrum sensing. Secondly, MME can be used to estimate the noise power as explained in Section 5.3. The estimated noise power is used by the ED to make the 2EMC fully-blind technique. Therefore, having the noise estimation part is a distinction of the 2EMC. Fig. 5.2 shows a schematic diagram of the 2EMC.

Setting-up the 2EMC

If a certain probability of false alarm has to be achieved by the 2EMC, then the parameters of both ED and MME stages have to be set accordingly. From (5.2)

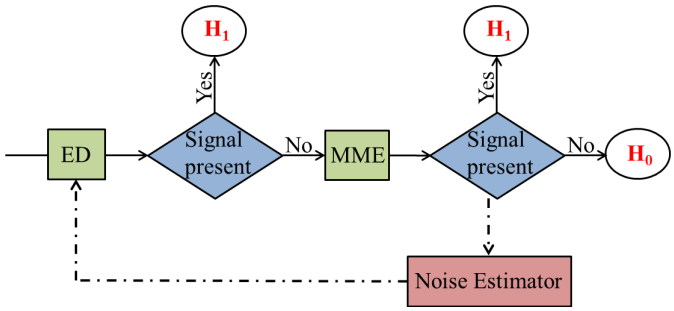

Figure 5.2: Schematic diagram of the 2EMC detector.

the probability of false alarm for the 2EMC denoted as p_f^C is obtained as

$$p_f^C = p_f^E + (1 - p_f^E)p_f^M. \tag{5.4a}$$

Subsequently, if a specific probability of false alarm is set for the ED aiming at a specific probability of false alarm for the 2EMC, then the probability of false alarm for the MME is calculated as

$$p_f^M = \frac{p_f^C - p_f^E}{1 - p_f^E}. \tag{5.4b}$$

Very high values of p_f^E, implies higher probabilities of detection and more usage of the ED as reflected by (3.2), (3.3) and (3.4). In return, this would make less efficient MME stage as its probability of false alarm will be too low and it will not be capable of detecting weak SNRs. In contrast, if p_f^E is too low, then the ED stage needs higher SNRs to detect, and therefore the decision will be mostly handed over to the MME, which in return, leads to a 2EMC with higher complexity. To compromise these two behaviours, a mid-way solution of having equal probabilities of false alarm of both ED and MME is applied. Consequently, by solving (5.4a), the probabilities of false alarm for both stages are found as

$$p_f^E = p_f^M = 1 - \sqrt{1 - p_f^C}. \tag{5.4c}$$

After setting p_f^E and p_f^M, the detection thresholds for both detectors are obtained using (3.3) and (3.10).

Signal Bandwidth Impact on 2EMC Performance

For the signal and observation bandwidth ratio, β, consideration, as explained in **Paper VIII** and Section 4.4, MME performance changes with β which satisfies the following relations

$$\arg\min_{\beta} \left(p_d^M\right) = [0, 1], \tag{5.5a}$$

$$\arg\max_{\beta}\left(p_d^M\right) = 0.5. \tag{5.5b}$$

For ED, as the signal energy increases when the signal bandwidth increases inside a specific bandwidth, then the probability of detection is a monotone function of β and can be written as

$$\arg\min_{\beta}\left(p_d^E\right) = 0, \tag{5.6a}$$

$$\arg\max_{\beta}\left(p_d^E\right) = 1. \tag{5.6b}$$

Since the performance of both ED and MME depends on the value of β, then for unknown β, 2EMC takes the advantages of each detector as evidenced by the simulations results shown in Fig. 5.3. Fig. 5.3 illustrates the regions of β where each detector performs better. The figure is generated considering -8 dB SNR WCDMA-like signal, $N = 5000, L = 20$, and $p_f^C = 0.1$. The values adopted in Fig. 5.3 ar used for illustrative purposes as a representative case. In general the same trends shown by Fig. 5.3 are valid for other values of SNR, N, L and p_f^C. As the figure shows, at very low values of β both detectors perform poorly. Yet, MME outperforms ED. Hence, with very low values of β, MME is the dominating detector of the 2EMC. In the middle range values of β, MME performs better than ED and still dominates the detection with more usage of the ED. Finally, at the high values of β, MME performance is poor while ED perform the best and serves as the dominating detector. As shown in the figure, the 2EMC always outperforms each detector individually.

5.3 Noise Variance Estimation

The relation between the white Gaussian noise variance and the minimum eigenvalue of the SCM is the base of different source separation algorithms such as Pisarenko and multiple signal classification (MUSIC) algorithms [89]. Based on this relation, the noise variance can be blindly estimated from the received signal. Extracting the noise variance from the received signal is the main idea behind MME. Therefore, MME can be used as a blind noise estimator. This blindly estimated noise variance can be fed back to the ED in order to make the 2EMC fully-blind detector as shown in Fig. 5.2.

The noise variance estimation by MME is mainly based on Marchenko Pastur density fitting for the noise eigenvalues. Therefore, the noise estimation process starts with splitting the two groups of eigenvalues representatives, namely signal and noise groups. The process of splitting the eigenvalues groups is explained in Section 4.4 where l, representing the number of signal plus noise eigenvalues, is estimated as $\hat{l}$ using (4.19). Thereafter, $\hat{\beta} = \hat{l}/L$ is computed. In Section 4.4 it has been shown that the two bounds of Marchenko Pastur density are noise variance, σ_z^2, dependant which results in having two equations and σ_z^2 as a single variable

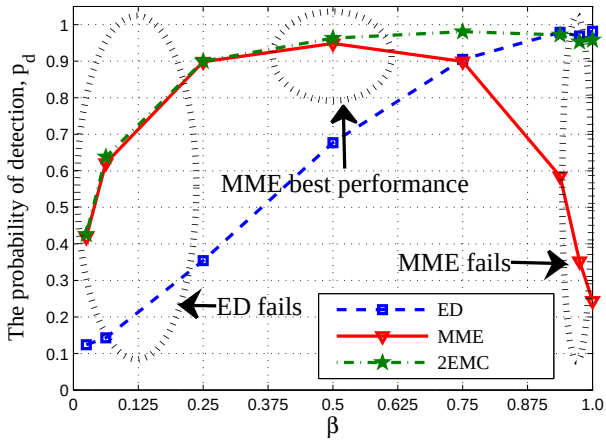

Figure 5.3: The probability of detection changes with β for ED, MME and 2EMC.

in both equations. Therefore, using each equation separately, two values of σ_z^2 call them σ_{z1}^2 and σ_{z2}^2 are obtainable as

$$\sigma_{z1}^2 = \frac{\lambda_L}{\left(1-\sqrt{c}\right)^2}, \tag{5.7a}$$

$$\sigma_{z2}^2 = \frac{\lambda_{\hat{l}+1}}{\left(1+\sqrt{c}\right)^2}, \tag{5.7b}$$

where λ_i denotes the SCM eigenvalue number i. Following that, K linearly spaced values between σ_{z1}^2 and σ_{z2}^2 denoted as π_k are generated as

$$\pi_k = \sigma_{z1}^2 + \left(\frac{k-1}{K-1}\right)\left(\sigma_{z2}^2 - \sigma_{z1}^2\right), 1 \leq k \leq K. \tag{5.8}$$

Consequently, K Marchenko Pastur densities of parameters $(1-\hat{\beta})c$ and π_k $\forall k$ are generated. The pdf of the noise group eigenvalues is obtained and then compared with the K Marchenko Pastur densities. The goodness of fit is used to pick the best $\pi(k)$ as an estimate of σ_z^2 denoted as $\hat{\sigma}_z^2$. The goodness of fit for each π_k, is denoted as D_k and obtained by

$$D_k = \left\| f(\lambda) - \mathcal{MP}\left((1-\hat{\beta})c, \pi_k\right)\right\|_2, 1 \leq k \leq K, \tag{5.9}$$

where $f(\lambda)$ is the pdf of the $(L-\hat{l})$ noise representatives eigenvalues and $\|.\|_2$ denotes the norm 2. The noise variance estimate is then given by

$$\hat{\sigma}_z^2 = \arg\min_{\pi_k}(D_k)). \tag{5.10}$$

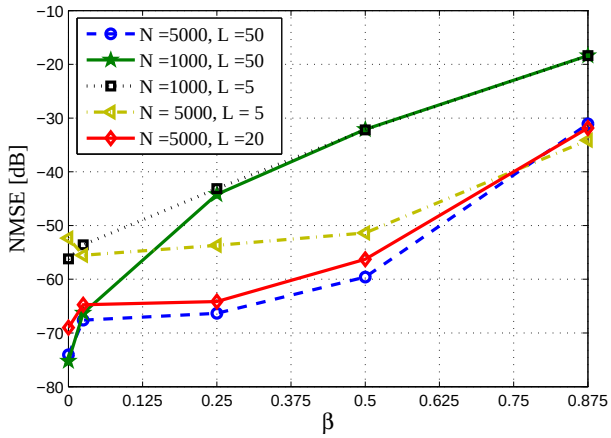

Figure 5.4: NMSE for the estimated noise using different values of N and L at different values of β.

To evaluate the noise estimation performance, Monte-Carlo simulations are carried out to compute the normalized mean square error (NMSE) between the actual and the estimated noise variance. The simulated noise variance is considered as the actual variance. The NMSE is calculated for different values of N, L and β. As shown in Fig. 5.4, the noise estimator performance is enhanced by increasing both N and L which is due to that more realizations are used for the estimation. Moreover, increasing β, decreases the estimator performance because with lower β, there exist more noise components and therefore the noise is estimated from higher number of eigenvalues representatives, $L - \hat{l}$.

Noise estimation by MME can also be used for other applications such as blind SNR estimation as in **Paper X**. In **Paper X**, the noise power is estimated by MME following the noise estimation procedure explained in the previous part of this section while the signal power is estimated from the mixture power by deduction the estimated noise power. Accordingly, a ratio between the estimated signal and noise powers is calculated as a blind estimate for the SNR.

Chapter 6

Conclusions and Future Recommendations

THERE has been increasing lack of resources in terms of radio spectrum to handle the recent enormously growing demand for wireless data traffic. One promising solution for this spectrum shortage is to open up some frequency bands for secondary access under cognitive radio and dynamic spectrum access framework. This thesis contributes in the area of dynamic spectrum access by means of studying spectrum sensing related aspects as an enabler for dynamic spectrum access. By spectrum sensing, the free of use frequency bands are found and can then be opportunistically utilized which contributes in making dynamic spectrum access omnipresent.

In this thesis, different challenges faced by spectrum sensing are studied. The challenges involved in the studies of this thesis are categorized into three categories, namely, blind spectrum sensing, sensing parameters optimization and primary users traffic modeling. Below are the concluding remarks drawn from the studies carried out in this thesis.

6.1 Concluding Remarks

In this thesis, two blind spectrum sensing techniques are developed. The first technique is based on discriminant analysis called spectrum discriminator (SD). The SD is a non-parametric technique used to split the noise and signal components in frequency domain. Moreover, to be able to deal with spectra that contains multiple PU signals with different SNRs, the SD is used as a basis for a multiple primary users peeling off technique. The second blind sensing technique developed in this thesis is a two-stage detector called 2EMC composed of energy detector (ED) and maximum-minimum eigenvalue detector (MME) as the first and second stage respectively. The second stage detection is used when the signal SNR is low

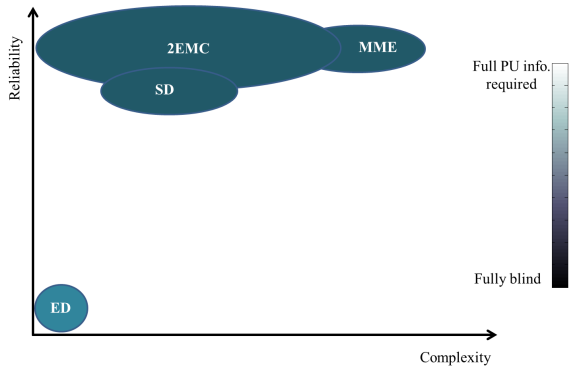

Figure 6.1: SD, 2EMC, ED and MME comparison.

and can not be detected by the first stage. Furthermore, the second stage is used as a noise estimator for the first stage.

A comparative study has been carried out among SD, 2EMC, ED and MME. The comparisons consider sensing reliability measured by the probabilities of false alarm and detection and the needed complexities measured in sensing times. Fig. 6.1 shows a general comparison of the pre-mentioned sensing techniques where the extent of blindness is color-coded and included in the comparison. As the figure depicts, SD performs blind, reliable and simple detection. On the other hand, 2EMC is a blind sensing technique with a higher reliability than the SD and largely varying complexity depending on the received SNR.

Regarding sensing optimization, the sensing time and periodic sensing interval are optimized mutually for ED with the aim of enhancing sensing reliability and increasing the utilization of the available opportunities. Furthermore, optimizing the periodic sensing intervals in a multi-channel sharing system where increasing the utilization of the whole sharing system spectrum is studied. Moving forward, a real-life sharing scenario of LTE cognitive femto-cell is considered for sensing intervals optimization with an objective of maximizing the femto-cell downlink throughput. Priori to solving the optimization problem in LTE cognitive femto-cells, an empirical statistical modeling for the LTE macro-cell channel occupancy is accomplished. The empirical modeling is based on fitting the length of both ON and OFF periods into a mixture of exponential distributions.

Under the umbrella of sensing optimization, MME limitation with ordinary time domain filtering is overcome by using frequency domain rectangular filtering where the signal spectrum shape is preserved. Moreover, the optimal ratio between the observation and occupation bandwidths for MME is analytically proven to be 0.5 with simulation verifications.

6.2 Future Recommendations

The studies of this thesis are centred around blind spectrum sensing, sensing optimization and primary traffic modeling. All addressed points are open for future research continuation. Following are some recommendations for further investigations regarding related aspects treated in this thesis.

Studying the feasibility and credibility of applying the spectrum sensing techniques developed in this thesis in different sharing scenarios and different applications is recommended. This also implies placing these techniques in a wider multidimensional landscape of the state of the art of spectrum sensing techniques. This wider multidimensionality can include, for example, the hardware complexity needed. For sensing parameters optimization, the optimization algorithms considered in this thesis can be further applicable for other sensing techniques apart from ED and MME which represents a direction of continuation. In the area of primary traffic modeling, investigating not only different primary systems, but also potential secondary systems is needed as a future research.

All the research performed within this thesis assumes single device spectrum sensing. Yet, the attained results can be used differently under cooperative spectrum sensing framework. As an example, the developed sensing techniques together with other existing techniques can be applied at different sensing devices and then their outcomes can be weighted differently for sensing fusion according to each technique reliability.

Moreover, the thesis considers the received signal characteristics impact on sensing performance. However, these received characteristics are associated with the transmitter side by means of the wireless channel properties which is not covered in the thesis. Therefore, it is recommended for the future studies to investigate different communication channel impacts on sensing performance. These communication channels include, but not limited to, multipath fading channels and fast fading channels.

Bibliography

[1] "Ericsson Mobility Report, Mobile Ttaffic Q3 2014," Tech. Rep., Nov. 2014.

[2] "IEEE Standard for Information technology - Telecommunications and information exchange between systems - Local and metropolitan area networks - Specific requirements. Part 15.3: Wireless Medium Access Control (MAC) and Physical Layer (PHY) Specifications for High Rate Wireless Personal Area Networks (WPANs) Amendment 2: Millimeter-wave-based Alternative Physical Layer Extension," *IEEE Std 802.15.3c-2009*, pp. c1–187, Oct. 2009.

[3] S. K. Yong and C.-C. Chong, "An overview of multigigabit wireless through millimeter wave technology: Potentials and technical challenges." *EURASIP J. Wireless Comm. and Networking*.

[4] "Report of the spectrum efficiency working group," FCC spectrum policy task force, Tech. Rep., 2002.

[5] "Notice of proposed rulemaking and order," FCC, FCC ET Docket 03-322, Tech. Rep., 2003.

[6] M. Wellens, J. Wu, and P. Mahonen, "Evaluation of spectrum occupancy in indoor and outdoor scenario in the context of cognitive radio," in *2nd Int. Conf. on Cognitive Radio Oriented Wireless Networks and Commun., (CrownCom)*, Aug. 2007, pp. 420 –427.

[7] I. Mitola, J., "Cognitive radio for flexible mobile multimedia communications," in *IEEE Int. Workshop on Mobile Multimedia Commun.*, 1999, pp. 3 –10.

[8] "Second memorandum opinion and order, in the matter of unlicensed operation in the TV broadcast bands and additional spectrum for unlicensed devices below 900 MHz and in the 3 GHz band," FCC, ET Docket 10-174, Tech. Rep., 2010.

[9] "Digital dividend: Cognitive access, statement in licence-exempting cognitive devices using interleaved spectrum," Ofcomm, Tech. Rep., Jul. 2009.

[10] "Technical and operational requirements for the possible operation of cognitive radio systems in the white spaces of the frequency band 470-790MHz," Electronic Communications Committee, Tech. Rep., Jan. 2011.

[11] IEEE802.22. [Online]. Available: http://www.ieee802.org/22/

[12] IEEE1900 group of standards. [Online]. Available: http://grouper.ieee.org/groups/dyspan/index.html

[13] M. Sherman, A. Mody, R. Martinez, C. Rodriguez, and R. Reddy, "IEEE standards supporting cognitive radio and networks, dynamic spectrum access, and coexistence," *IEEE Commun. Mag.*, vol. 46, no. 7, pp. 72 –79, Jul. 2008.

[14] "Front matter," in *Cognitive Radio Communications and Networks*, A. M. W. N. T. Hou, Ed. Oxford: Academic Press, 2010. [Online]. Available: http://www.sciencedirect.com/science/article/pii/B9780123747150005001

[15] M. Song, C. Xin, Y. Zhao, and X. Cheng, "Dynamic spectrum access: from cognitive radio to network radio," *IEEE Wireless Commun.*, vol. 19, no. 1, pp. 23–29, Feb. 2012.

[16] C. Xin, M. Song, L. Ma, G. Hsieh, and C.-C. Shen, "Network coding relayed dynamic spectrum access," in *Proceedings of the ACM Workshop on Cognitive Radio Networks(CoRoNet).*

[17] J. Peha, "Sharing spectrum through spectrum policy reform and cognitive radio," *Proceedings of the IEEE*, vol. 97, no. 4, pp. 708–719, Apr. 2009.

[18] S. Haykin, "Cognitive radio: brain-empowered wireless communications," *IEEE J. Sel. Areas Commun.*, vol. 23, no. 2, pp. 201 – 220, Feb. 2005.

[19] T. Yucek and H. Arslan, "A survey of spectrum sensing algorithms for cognitive radio applications," *IEEE Commun. surveys Tutorials*, vol. 11, no. 1, pp. 116 –130, 2009.

[20] A. Ghasemi and E. Sousa, "Spectrum sensing in cognitive radio networks: requirements, challenges and design trade-offs," *IEEE Commun. Mag.*, vol. 46, no. 4, pp. 32 –39, Apr. 2008.

[21] D. Ariananda, M. Lakshmanan, and H. Nikoo, "A survey on spectrum sensing techniques for cognitive radio," in *Int. Workshop on Cognitive Radio and Advanced Spectrum Management*, May 2009, pp. 74 –79.

[22] M. Nekovee, T. Irnich, and J. Karlsson, "Worldwide trends in regulation of secondary access to white spaces using cognitive radio," *IEEE Wireless Commun. Mag.*, vol. 19, no. 4, pp. 32 –40, Aug. 2012.

[23] "Measurements on the performance of the DVB-T receivers in the presence of the interference from the mobile service (especially from LTE)„" Tech. Rep.

[24] "Dynamic frequency selection (DFS) in wireless access systems including radio local area networks for the purpose of protecting the radiodetermination service in the 5 GHz band," Inetnational Telecommunication Union, Tech. Rep., 2003.

[25] "Spectrum sharing in the 5 GHz band DFS best practices," Spectrum & Regulatory Committee, Spectrum Sharing Task Group, Tech. Rep., Oct. 2007.

[26] "Technical impact on existing primary services in the band 2700-2900 MHz due to the proposed introduction of new systems," Electronic Communications Commitee, Tech. Rep., Jun. 2002.

[27] A. Brandao, J. Sydor, W. Brett, J. Scott, P. Joe, and D. Hung, "5 GHz RLAN interference on active meteorological radars," in *IEEE 61st Vehicular Technology Conf.*, vol. 2, May-Jun. 2005, pp. 1328 – 1332 Vol. 2.

[28] M. Hamid and N. Björsell, "Geo-location spectrum opportunities database in downlink radar bands for OFDM based cognitive radios," *IEEE Conf. on Commun., Science and Information Engineering (CCSIE)*, pp. 39–43.

[29] K. W. Sung, E. Obregon, and J. Zander, "On the requirements of secondary access to 960 -1215 MHz aeronautical spectrum," in *IEEE Symp. on New Frontiers in Dynamic Spectrum Access Networks (DySPAN)*, May 2011, pp. 371 –379.

[30] A. Attar, O. Holland, M. Nakhai, and A. Aghvami, "Interference-limited resource allocation for cognitive radio in orthogonal frequency-division multiplexing networks," *IET Commun.*, vol. 2, no. 6, pp. 806 –814, Jul. 2008.

[31] T. Brown, "An analysis of unlicensed device operation in licensed broadcast service bands," in *1st IEEE Int. Symp. on New Frontiers in Dynamic Spectrum Access Networks (DySPAN)*, nov. 2005, pp. 11 –29.

[32] H. Urkowitz, "Energy detection of unknown deterministic signals," *Proceedings of the IEEE*, vol. 55, no. 4, pp. 523 – 531, April 1967.

[33] R. Tandra and A. Sahai, "SNR walls for signal detection," *IEEE J. of Sel. Topics Signal Process.*, vol. 2, no. 1, pp. 4 –17, Feb. 2008.

[34] A. Mossaa and V. Jeoti, "Cognitive radio: Cyclostationarity-based classification approach for analog TV and wireless microphone signals," in *Innovative Technologies in Intelligent Systems and Industrial Applications (CITISIA)*, Jul. 2009, pp. 107 –111.

[35] D. Cabric, "Addressing feasibility of cognitive radios," *IEEE Signal Process. Mag.*, vol. 25, no. 6, pp. 85 –93, Nov. 2008.

[36] S. Kapoor, S. Rao, and G. Singh, "Opportunistic spectrum sensing by employing matched filter in cognitive radio network," in *Int. Conf. Commun. Systems and Network Technologies (CSNT)*, Jun. 2011, pp. 580 –583.

[37] S. M. Kay, *Fundamentals of Statistical Signal Processing*, 5th ed. Prentice Hall, 2004, pp. 487 – 488.

[38] S. Mishra, S. ten Brink, R. Mahadevappa, and R. Brodersen, "Cognitive technology for Ultra-Wideband/Wimax coexistence," in *2nd IEEE Int. Symp. on New Frontiers in Dynamic Spectrum Access Networks (DySPAN)*, Apr. 2007, pp. 179 –186.

[39] Y. Zeng and Y. chang Liang, "Eigenvalue-based spectrum sensing algorithms for cognitive radio," *IEEE Trans. Commun.*, vol. 57, no. 6, pp. 1784 –1793, Jun. 2009.

[40] ——, "Maximum-minimum eigenvalue detection for cognitive radio," in *IEEE 18th Internat. Symp. Personal, Indoor and Mobile Radio Commun.*, Sep. 2007, pp. 1–5.

[41] R. Zhang, T. J. Lim, Y.-C. Liang, and Y. Zeng, "Multi-antenna based spectrum sensing for cognitive radios: A GLRT approach," *IEEE Trans. Commun.*, vol. 58, no. 1, pp. 84–88, Jan. 2010.

[42] A. Taherpour, M. Nasiri-Kenari, and S. Gazor, "Multiple antenna spectrum sensing in cognitive radios," *IEEE Trans. Wireless Commun.*, vol. 9, no. 2, pp. 814–823, Feb. 2010.

[43] M. Shakir, W. Tang, A. Rao, M. Imran, and M.-s. Alouini, "Eigenvalue ratio detection based on exact moments of smallest and largest eigenvalues," in *6th Int. ICST Conf. on Cognitive Radio Oriented Wireless Networks and Commun. (CROWNCOM)*, Jun. 2011, pp. 46–50.

[44] W. Zhang, G. Abreu, M. Inamori, and Y. Sanada, "Spectrum sensing algorithms via finite random matrices," *IEEE Trans. Commun.*, vol. 60, no. 1, pp. 164–175, Jan. 2012.

[45] U. Y. Mohamad and D. Dahlhaus, "Cognitive radio sensing based on joint distribution of pseudo wishart matrix eigenvalues," in *Wireless Telecommun. Symp. (WTS)*, Apr. 2014, pp. 1–6.

[46] Z. Sun, W. Han, Z. Li, Y. Zhang, and M. Lin, "Spectrum sensing method without the impact of noise uncertainty," in *IEEE Global Conf. on Signal and Information Process. (GlobalSIP)*, Dec. 2013, pp. 1166–1169.

[47] P. Kolodyz, "Dynamic spectrum policies: Promises and challenges," *J. commun. law and policy*, vol. 22, no. 2, pp. 201 – 220, Feb. 2004.

[48] L. Shen, H. Wang, W. Zhang, and Z. Zhao, "Blind spectrum sensing for cognitive radio channels with noise uncertainty," *IEEE Trans. Wireless Commun.*, vol. 10, no. 6, pp. 1721 –1724, Jun. 2011.

[49] N. Khajavi, S. Sadeghi, and S.-S. Sadough, "An improved blind spectrum sensing technique for cognitive radio systems," in *5th Int. Symp. on Telecommun. (IST)*, Dec 2010, pp. 13 –17.

[50] R. Wang and M. Tao, "Blind spectrum sensing by information theoretic criteria for cognitive radios," *IEEE Trans. Veh. Technol.*, vol. 59, no. 8, pp. 3806 –3817, Oct. 2010.

[51] F. Xu, J. Hui, X. Zheng, and Z. Zhou, "Accurate blind spectrum sensing based on high order statistical analysis in cognitive radio system," in *IEEE Int. Conf. Commun. Technol. and Applications (ICCTA)*, Oct. 2009, pp. 386 –391.

[52] H. Jiang, L. Lai, R. Fan, and H. Poor, "Optimal selection of channel sensing order in cognitive radio," *IEEE Trans. on Wireless Commun.*, vol. 8, no. 1, pp. 297 –307, Jan. 2009.

[53] A. Ewaisha, A. Sultan, and T. ElBatt, "Optimization of channel sensing time and order for cognitive radios," in *IEEE Conf. Wireless Commun. and Networking (WCNC)*, Mar. 2011, pp. 1414 –1419.

[54] W.-Y. Lee and I. Akyildiz, "Optimal spectrum sensing framework for cognitive radio networks," *IEEE Trans. Commun.*, vol. 7, no. 10, pp. 3845 –3857, Oct. 2008.

[55] H. N. Pham, Y. Zhang, P. Engelstad, T. Skeie, and F. Eliassen, "Energy minimization approach for optimal cooperative spectrum sensing in sensor-aided cognitive radio networks," in *5th Annu ICST Wireless Internet Conf. (WICON)*, Mar. 2010, pp. 1 –9.

[56] Y.-C. Liang, Y. Zeng, E. Peh, and A. T. Hoang, "Sensing-throughput tradeoff for cognitive radio networks," *IEEE Trans. Wireless Commun.*, vol. 7, no. 4, pp. 1326–1337, Apr. 2008.

[57] D. Hong and S. Rappaport Stephen, "Traffic model and performance analysis for cellular mobile radio telephone systems with prioritized and nonprioritized handoff procedures," *IEEE Trans. Veh. Technol.*, vol. 35, no. 3, pp. 77–92, Aug. 1986.

[58] R. Guerin, "Channel occupancy time distribution in a cellular radio system," *IEEE Trans. Veh. Technol.*, vol. 36, no. 3, pp. 89–99, Aug. 1987.

[59] M. Wellens, J. Riihijärvi, and P. Mähönen, "Empirical time and frequency domain models of spectrum use," *Phys. Commun.*, vol. 2, no. 1-2, pp. 10–32, Mar. 2009.

[60] E. Yavuz and V. C. M. Leung, "Computationally efficient method to evaluate the performance of guard-channel-based call admission control in cellular networks," *IEEE Trans. Veh. Technol.*, vol. 55, no. 4, pp. 1412–1424, Jul. 2006.

[61] H. Kim and K. Shin, "Efficient discovery of spectrum opportunities with MAC-layer sensing in cognitive radio networks," *IEEE Trans. Mobile Computing*, vol. 7, no. 5, pp. 533 –545, May 2008.

[62] M. Khoshkholgh, K. Navaie, and H. Yanikomeroglu, "Novel approaches to determine the optimal operating point of spectrum sensing in overlay spectrum sharing," pp. 1–5, 2010.

[63] H. Holma and A. Toskala, *WCDMA for UMTS: HSPA Evolution and LTE*. New York, NY, USA: John Wiley & Sons, Inc., 2007.

[64] M. Mehta, *Random Matrices*. Elsevier Science, 2004.

[65] R. Couillet and M. Debbah, *Random Matrix Methods for Wireless Communications*. Cambridge University Press, 2011.

[66] C. A. Tracy and H. Widom, "On orthogonal and symplectic matrix ensembles," *Commun. Math. Phys.*, pp. 727–754, 1996.

[67] ——, "The distribution of the largest eigenvalue in the Gaussian ensembles," in *Calogero-Moser-Sutherland models CRM Ser. Math. Phys.* Springer, 2000, pp. 461–472.

[68] R. A. Fisher, "The use of multiple measurements in taxonomic problems," *Ann Eugenics*, vol. 7, pp. 179 –188, 1936.

[69] K. Barbé and W. Van Moer, "Automatic detection, estimation, and validation of harmonic components in measured power spectra: All-in-one approach," *IEEE Trans. Instrum. Meas.*, vol. 60, no. 3, pp. 1061 –1069, Mar. 2011.

[70] A. Feldmann and W. Whitt, "Fitting mixtures of exponentials to long-tail distributions to analyze network performance models," 1997, pp. 245–279.

[71] H. Akaike, "A new look at the statistical model identification," *IEEE Trans. Autom. Control*, vol. 19, no. 6, pp. 716–723, Dec. 1974.

[72] D. Knisely, T. Yoshizawa, and F. Favichia, "Standardization of femtocells in 3GPP," *IEEE Commun. Mag.*, vol. 47, no. 9, pp. 68–75, Sep. 2009.

[73] O. Gharehshiran, A. Attar, and V. Krishnamurthy, "Collaborative sub-channel allocation in cognitive lte femto-cells: A cooperative game-theoretic approach," *IEEE Trans. Commun.*, vol. 61, no. 1, pp. 325–334, Jan. 2013.

[74] S. Al-Rubaye, A. Al-Dulaimi, and J. Cosmas, "Cognitive femtocell," *IEEE Veh. Technol. Mag.*, vol. 6, no. 1, pp. 44–51, Mar. 2011.

[75] A. Adhikary, V. Ntranos, and G. Caire, "Cognitive femtocells: Breaking the spatial reuse barrier of cellular systems," in *Inform. Theory and Applicat. Workshop (ITA)*, Feb. 2011, pp. 1–10.

[76] M. Buddhikot, "Cognitive radio, DSA and self-X: Towards next transformation in cellular networks."

[77] "Evolved universal terrestrial radio access (E-UTRA); Further advancements for E-UTRA physical layer aspects, release 09," *3GPP Standard: 3GPP TR 36.814*, pp. 93–96, Mar. 2010.

[78] S. Park, W. Seo, Y. Kim, S. Lim, and D. Hong, "Beam subset selection strategy for interference reduction in two-tier femtocell networks," *IEEE Trans. Wireless Commun.*, vol. 9, no. 11, pp. 3440–3449, Nov. 2010.

[79] R. Nadakuditi and A. Edelman, "Sample eigenvalue based detection of high-dimensional signals in white noise using relatively few samples," *IEEE Trans. Signal Process.*, vol. 56, no. 7, pp. 2625–2638, 2008.

[80] A. Edelman and R. Nadakuditi, "Random matrix theory," *Acta Numerica.*, vol. 14, no. 7, pp. 233–297, 2005.

[81] V. A. Marchenko and L. A. Pastur, "Distribution of eigenvalues for some sets of random matrices," *Math.of the USSR-Sbornik.*, vol. 1, no. 4, pp. 457–483, 1967.

[82] M. Wax and T. Kailath, "Detection of signals by information theoretic criteria," *IEEE Trans. Acoust., Speech, Signal Process.*, vol. 33, no. 2, pp. 387–392, Apr. 1985.

[83] W. Ejaz, N. ul Hasan, and H. Kim, "SNR-based adaptive spectrum sensing for cognitive radio networks," vol. 8, no. 9, pp. 6095–6105, Sep. 2012.

[84] P. Nair, A. Vinod, K. Smitha, and A. Krishna, "Fast two-stage spectrum detector for cognitive radios in uncertain noise channels," *IET Commun.*, vol. 6, no. 11, pp. 1341–1348, Jul. 2012.

[85] "Combined energy detection and one-order cyclostationary feature detection techniques in cognitive radio systems," *J. China Universities of Posts and Telecommun.*, vol. 17, no. 4, pp. 18 – 25, 2010.

[86] S. Geethu and G. Narayanan, "A novel high speed two stage detector for spectrum sensing," *Procedia Technology*, vol. 6, no. 0, pp. 682 – 689, 2012.

[87] S. Maleki, A. Pandharipande, and G. Leus, "Two-stage spectrum sensing for cognitive radios," in *IEEE Int. Conf. Acoustics Speech and Signal Process. (ICASSP)*, Mar. 2010, pp. 2946–2949.

[88] K. Smitha, A. Vinod, and P. Nair, "Low power DFT filter bank based two-stage spectrum sensing," in *Int. Conf. on Innovations in Information Technology (IIT)*, Mar. 2012, pp. 173–177.

[89] M. H. Hayes, "Statisticl digital signal processing and modeling," *John Wiley & Sons, INC*, vol. 1, pp. 459–465, 1996.

Part II

Included Publications